UiT The Arctic University of Norway

The Norwegian College of Fishery Science, UiT The Arctic University of Norway

Securidine analogues from the marine bryozoan *Securiflustra securifrons*

Daniel Salamonsen

Master's thesis in Marine Biotechnology [BIO-3901] (May 2021)

Abstract

Bioprospecting of natural products has been performed in various manners throughout the ages and has become key to human development and prolonged survival, exemplified by the inventions of antibiotics, vaccines and numerous pharmaceuticals. The terrestrial environment has been scoured for natural resources for centuries, while a massive unexploited potential for chemical diversity resides in our marine habitats.

The aim of this thesis was to isolate, elucidate and characterize securidine analogues and other novel compounds from the marine bryozoan *Securiflustra securifrons.* The work was based on an earlier project at Marbio were the mono-brominated alkaloid Securidine A had been isolated from an aqueous extract of *S. securifrons*.

Two aqueous extracts of *S. securifrons* were dereplicated using ultra-high performance liquid chromatography (UHPLC) coupled with electrospray ionization high-resolution mass spectrometry (ESI-HR-MS) in order to narrow down the list of potential candidates for isolation. Securidine A was successfully isolated alongside four novel compounds from the extracts using mass-guided fractionation. Structure elucidation was performed by nuclear magnetic resonance (NMR) experiments (^{1}H, ^{13}C, HMBC, HSQC and COSY) and by analyzing fragmentation patterns from the ionization of the compounds using HR-MS. The complete structures of two novel securidine analogues (MBC-340 and MBC-342) were elucidated during this work, while partial structures of two compounds (MBC-339 and MBC-341) were obtained. Bioactivity characterization revealed some cytotoxic effect of the securidine analogue MBC-340 against the human melanoma cancer cell line A2058. No antibacterial, antifungal, antidiabetic or antibiofilm formation effects were detected at the tested concentration of 50 µM.

The results from this thesis shows that secondary metabolites from bryozoans are a rich source of novel chemistry and demonstrates the possibility to discover bioactive properties in analogues of known compounds with only minor chemical differences.

Acknowledgements

The work presented in this thesis was conducted at Marbio (Norwegian College of Fisheries) from August 2020 to May 2021. Some experimental work was also performed at the Department of Chemistry at UiT - The Arctic University of Norway.

I would like to thank my supervisors Espen Hansen, Jeanette Hammer Andersen and especially my main supervisor Kine Østnes Hansen for all guidance, knowledge, encouragement and motivation during my work. It has been an unpredictable year due to the circumstances, but through structured planning and great cooperation the work was finished in time for the original deadline.

I would also like to thank Yannick Schneider for his help and education in isolation techniques and structure elucidation, as well as Marte Albrigtsen and Kirsti Helland for their assistance with the bioactivity characterization. Thanks to Johan Isaksson at the Department of Chemistry for performing the NMR work.

Tromsø, May 2021
Daniel Salamonsen

Abbreviations

1D	One-dimensional
2D	Two-dimensional
A	Mobile phase A (ddH_2O with 0.1% FA)
ACN	Acetonitrile
B	Mobile phase B (ACN with 0.1% FA)
BHI	Brain heart infusion
BPI	Base peak intensity
BSA	Bovine serum albumin
CCS	Collision cross section
CFU	Colony forming units
COSY	Correlated spectroscopy
ddH_2O	Double-distilled water (Milli-Q®)
DiFMUP	6,8-difluoro-4-methylumbelliferyl phosphate
D-MEM	Gibco Dulbecco's Modified Eagle Medium
DMSO	Dimethyl sulfoxide
EDTA	Ethylenediaminetetraacetic acid
ESI	Electrospray ionization
eV	Electron volt
FA	Formic acid
FBS	Fetal bovine serum
h	Hour(s)
HEPES	4-(2-hydroxyethyl)-1-piperazineethanesulfonic acid
HMBC	Heteronuclear multiple bond correlation
HMQC	Heteronuclear multiple quantum correlation

HPLC	High performance liquid chromatography
HR	High resolution
IC_{50}	Half-maximal inhibitory concentration
MEM	Minimum Essentials Medium Eagle
MeOH	Methanol
MH	Mueller-Hinton broth
MIC	Minimum inhibitory concentration
min	Minutes
MOPS	3-(*N*-morpholino)propanesulfonic acid
MS	Mass spectrometry
MTS	3-(4,5-dimethylthiazol-2-yl)-5-(3-carboxymethoxyphenyl)-2-(4-sulfophenyl)-2H-tetrazolium
m/z	Mass-to-charge
NaCl	Sodium chloride
NMR	Nuclear magnetic resonance
NOESY	Heteronuclear Overhauser effect
PDB	Potato dextrose broth
ppm	Parts per million
PTP1B	Protein tyrosine phosphatase 1B
rpm	Rounds per minute
RPMI	Gibco Roswell Park Memorial Institute
RT	Retention time
TIC	Total ion current
UHPLC	Ultra-high performance liquid chromatography

Table of Contents

1 Introduction

1.1 Bioprospecting

Humans have always used natural resources for survival and development in terms of food, clothing, shelter and tools, as well as medicine. Analysis of dental evidence has suggested that Neanderthals chewed on bitter-tasting plants, thereby ingesting salicylic acid. Today, the acetylated analogue of salicylic acid is still used as the active ingredient in aspirin (Weyrich et al., 2017). The first recorded instance of a medical prescription dates to around 2000 B.C from the Third Dynasty of Ur in ancient Mesopotamia (Biggs, 2005). Throughout the years, much of our medicinal understanding has been based upon application of natural resources, such as plant and fungi, to heal injuries and alleviate suffering. Traditional plant-based medicine is still common practice worldwide and an integral part of the health system in several countries, often used in combination with modern chemistry-based medicine (Thomford et al., 2015; Huang et al., 2018; Appiah et al., 2018). The constant search for knowledge regarding the utilization of natural assets has been crucial for human development and prolonged survival, which has resulted in the creation of essentials such as antibiotics, analgesics and vaccines. Today, the field of study that covers natural products is immensely broad, within which bioprospecting plays an important role.

Bioprospecting is defined as the targeted and systematic search for natural products, such as bioactive small molecules, macromolecules or genetic information, with the purpose of developing commercially viable products (Mateo et al., 2001; Tamayo et al., 2004). The products emerging through bioprospecting can be applied to numerous industries in form of pharmaceuticals, nutraceuticals, agriculture, aquaculture, nanotechnology, bioremediation, cosmetics and medical engineering amongst others (Mateo et al., 2001; Beattie et al., 2011). Feasible products can potentially emanate from a plethora of organisms, from common plants and fungi traditionally applied in medicine to still undiscovered marine invertebrates and microorganisms at the ocean's depth. Bioprospecting can be carried out based on both applied and basic research. When applied research is conducted, the aim is to seek answers and solutions to a practical issue, such as drug development to treat a specific disease. The basic research approach is mainly driven by curiosity and seeks to expand scientific knowledge,

rather than attempting to solve specific problems (Amon, 2015). Often, there is no definitive barrier between applied or basic research in terms of bioprospecting since the outcome and result of the scientific project can vary greatly. Some bioprospecting efforts will merely lead to increased knowledge about chemical diversity and natural interactions, while others may yield viable natural products and commercialization, regardless of the initial motive and research approach.

1.1.1 Natural products

Natural products, in the broadest definition, refers to all chemical compounds that are produced by living organisms and naturally found in nature. Searching for natural products is an effective way to discover novel compounds and new chemical scaffolds and properties. Nature inhibits a far superior chemical diversity compared to what we are currently able to efficiently synthesize in laboratories. This is due to evolutionary selection, which have designed highly specified and potent compounds throughout millions of years (Paterson & Anderson, 2005).

Natural products can be separated into two main categories: primary and secondary metabolites. Primary metabolites such as fatty acids, carbohydrates and amino acids, are directly involved in vital processes including normal growth, development and reproduction. Primary metabolites are highly conserved in structure and function across multiple species. Secondary metabolites are small molecules that are not directly involved in crucial metabolic processes, but mainly serve as means to increase an organism's survivability and reproducing ability (Thoma et al., 2020). As opposed to primary metabolites, they are often exclusively expressed under certain conditions. The natural functions of secondary metabolites are many. They may function as toxic compounds to deter predators or combat pathogens as complementation to a weak or absent adaptive immune system, contribute to aesthetic changes, act as metal transporters or as differentiation signals. In addition, they may increase symbiotic interactions and environmental adaptations, or serve as sexual attractants and hormones (Demain & Fang, 2000; Petersen et al., 2020). Secondary metabolites are often specific for a single species or a small monophyletic group, which leads to huge diversity in terms of chemical structures and functions. This makes

secondary metabolites highly interesting for bioprospecting purposes and commercialization, such as development of new lead compounds, pharmaceuticals, nutraceuticals and insecticides.

The utilization of natural products has been vastly successful in terms of drug discovery and development. Over the last four decades, from 1981 to 2019, only 24.6% of all approved drugs are totally synthetic, often found by screening or modification of an already existing agent (Newman & Cragg, 2020). The updated fifth edition from Newman and Craggs comprehensive review of new drugs classifies the origins of 1881 approved drugs according to seven major categories and two subcategories. Out of the drugs included in the review, 41.9% are either an unaltered biological product or a natural product derivative. Natural product mimics compromises 22.5% of the drugs, while synthetic drugs, where the active pharmacophore is naturally derived, constitutes 3.2% of all drugs (see Figure 1). The review highlights the continued importance of natural products in drug discovery and urges to improve funding systems and conjunctive efforts with synthetic biology, especially regarding discovery of novel antibiotics and antifungal drugs (Newman & Cragg, 2020).

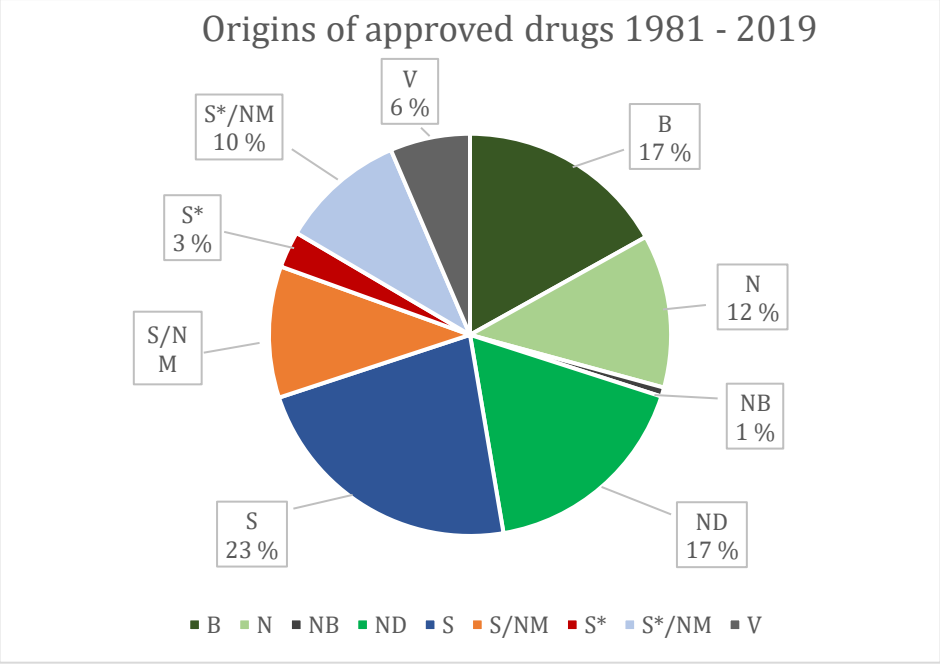

Figure 1 - The origin of approved drugs from 1981 - 2019 according to Newman & Cragg (2020)*; n = 1881. B: Biological (usually large peptide or protein), N: Natural product, NB: Natural botanical product, ND: Natural product derivative, S: Synthetic product, S*: Synthetic products with pharmacophore from a natural product, NM: Natural product mimic, V: vaccine.*

However, natural products-based drug discovery is not without challenges (see 1.1.8 - challenges in marine bioprospecting). The need for substantial investment due to a long and complex development time made major companies consider the practice as too costly and financially treacherous (Ventola, 2015; Atanasov et al., 2015; Newman & Cragg, 2020). The combination of various issues, in addition to the developments in combinatorial and computational techniques, led to a decreased interest for investments in natural products drug discovery and the industry gradually shifted towards high-throughput sequencing of synthetic compound libraries introduced in the 1990s (Bernardini et al., 2018; Atanasov et al., 2015). Nevertheless, this new approach did not yield the expected results and consequently the approval rates of new drugs declined.

As of yet, compounds found in synthetic libraries cannot outcompete natural product libraries in terms of chemical diversity (Feher & Schmid, 2003; Koehn & Carter, 2005). Comparisons of the chemical properties and diversity of natural products have shown to be more aligned with the chemical features of drugs, compared to compounds found in synthetic libraries (Blunt et al., 2018). Natural products generally have higher molecular weight, number of chiral centers, heavy atoms, rings structures and hydrogen-bond donors and acceptors, as well as being less lipophilic and more saturated (Feher & Schmid, 2003; Muigg et al., 2013). Generally, an increased number of chiral centers, lower molecular flexibility and larger molecular size is beneficial for receptor specificity and potency (Feher & Schmid, 2003). They also possess other optimized properties, such as high binding affinity to specific target proteins, often protein domains conserved through evolution (Appendino et al., 2010). Furthermore, natural products possess a wide range of pharmacophores and high degree of stereochemistry (Harvey et al., 2015). In addition to the chemical properties related to the pharmacodynamic capacity of natural products, they are also shown to have better pharmacokinetic properties *in vivo*. There are several reasons for this which includes that their natural origin makes them likely to be substrates for transporter systems in the human body (Harvey et al., 2015). This is highly beneficial since most therapeutics work on intracellular targets and must therefore pass through biological membranes to exert activity. These attributes make adaptable natural products a great starting point for development of new therapeutic derivatives.

To accommodate and exploit recent technological advancements, the traditional bioassay-guided approach has been modified in various ways. Prefractionation to improve applicability, pre-filtering of screening libraries, application of "omic" approaches and other combinatorial methods are some adjustments incorporated to improve efficiency and keep natural drug discovery innovative (Harvey et al., 2015; Maghembe et al., 2020).

1.1.2 The marine environment

Historically, the focus of bioprospecting has mainly been on terrestrial habitats due to its easy accessibility. As a natural consequence, most approved drugs based on natural products are derived from terrestrial plants, fungi or microorganisms. As of today, only 15 approved drugs on the international market comes from the marine environment (Mayer et al., 2020). This amounts to a tiny percentage when compared to the total amount of FDA approved drugs, which were determined to be 1453 drugs as of 2013 (Patridge et al., 2015), as well as 361 new approvals between 2008 and 2018 (Batta et al., 2020).

Oceans cover around 70% of the total surface of the Earth and the marine environments are home to around 95% of the total biosphere (Altmann, 2017). In addition to its sheer size, the marine environment possesses tremendous diversity in terms of habitats and ecosystems due to both biotic and abiotic factors such as temperature, salinity, pressure, currents, competition, access to food and light etc. Due to these variations, there are many unique and adapted species with highly modified enzymes and metabolites. Some examples of such adaptions are cold-adapted enzymes in Arctic and Antarctic regions, salt tolerant microorganisms in high-salinity oceans and bioluminescence in organisms living in the deep, dark sea (Debashish et al., 2005; Duarte et al., 2018; Vacher et al., 2018). These adaptations provide a great foundation for chemical diversity and discovery of novel and complex compounds. The massively skewed distribution of approved terrestrial-derived pharmaceuticals compared to marine-derived, points to a huge and unexploited potential in organisms living below the littoral zone. As technological advancements of equipment and techniques continue rapidly, the marine environment has for the last decades been more accessible than ever for scientists.

Life as we know it originally begun in the ocean and have gone through natural selection for billions of years. This have led to an enormous biodiversity and an even bigger chemical diversity. There are over 30 000 known compounds from the marine environment and since 2008 over 1000 new compounds are discovered yearly (Lindequist, 2016). The World Register of Marine Species (WoRMS) operates with about 238 150 accepted marine species (per May 2021), but some scientists have estimated that up to 90% of all marine species are yet to be discovered or described (Lindequist, 2016).

1.1.3 Marine secondary metabolites

Pharmaceuticals deriving from the marine environment looks to be on the rise. From the 14 approved marine drugs on the market, four of them (Polivy™, PADCEV™, Zepzelca™ and Blenrep™) have been approved since 2019 (Mayer et al., 2020). This is a small sample size, but the fact that almost 1/3 of all approved marine drugs have been authorized in the last two years is promising for the marine bioprospecting field. Nine out of the 14 drugs, including all the recent approvals, are antineoplastic drugs for various types of cancer (Mayer et al, 2020). The trend continues into the clinical trials, where 13 out of 16 drugs in phase II and III are anticancer drugs. Even though the main focus seems to be on antineoplastic agents, marine secondary metabolites have plenty of other well-documented bioactivities, including antimicrobial, antifungal and antiviral effects to name a few (Petersen et al., 2020)

1.1.3.1 Why are secondary metabolites produced?

Secondary metabolites often serve an ecological purpose for the producing species but can also act in response to external stimuli or simply be conserved though evolution (Nielsen et al., 2019; Kurosaki, 2012). As mentioned, secondary metabolites are not essential, but generally increases the survivability, reproducibility or competitiveness of the species. One example of secondary metabolites enhancing survivability and competitiveness comes from marine cone snails. These gastropod mollusks are able to produce one of the most potent toxins found in nature, called conotoxins. The toxins are used to hunt down and paralyze prey to compensate

for their slow movement (Morales Duque et al., 2019). The neuroactive peptide ziconotide (trademark Prialt®), which was FDA approved as a non-opioid analgesic for chronic pain in 2004, derives from an omega-conotoxin from *Conus magus* (Miljanich, 2004). The high potency of conotoxins is likely due to the fact that the concentration is quickly diluted in water when released, which implies that marine secondary metabolites needs to be exceedingly potent in order to have the desired effect (Haefner, 2003).

1.1.3.2 Why are secondary metabolites bioactive?

There exists a huge variety of chemical classes amongst marine secondary metabolites. Some of the most prominent chemical classes linked with bioactivity include peptides, steroids, terpenoids, alkaloids and polyketides (Loureiro et al., 2019). Some organisms produce a broad collection of secondary metabolites, but not all of them are confirmed to be bioactive through testing. Why are seemingly some secondary metabolites bioactive while others aren't? One theory could be that organisms often produce a multitude of similar molecules, to increase the likelihood that some compounds exhibit the desired effect. These compounds will themselves adapt through evolution and become more potent and efficient, leaving other derivatives futile. Another rationale could be that most secondary metabolites are in fact bioactive in nature and during warranted circumstances, but our ability (and willingness) to replicate these conditions are limited and dependent on time and resources.

The ability of some organisms to produce a wide range of bioactive secondary metabolites grants them a selective advantage against competitors and better opportunities for adaption to environmental challenges (Petersen et al., 2020). A functioning array of secondary metabolites is especially important for the survival of sessile organisms. Since these organisms are immobile and unable to escape from predators, pathogens, overgrowth or environmental changes, they need other types of defensive mechanisms. Marine invertebrates, such as phyla Porifera, Tunicata and Bryozoa are examples of sessile organisms that, through their long existence, have developed complex chemical defense systems. It has also been discovered that in many instances, it is not the organism itself that produces the secondary metabolites, but rather symbiotic microorganisms that lives alongside the invertebrate (Choudhary et al., 2017).

One prominent example of this is the drug trabectedin (trademark Yondelis®) that was approved in 2015. Trabectedin is an alkaloid isolated from the tunicate *Ecteinascidia turbinata*, which is used in treatment for soft tissue sarcoma and ovarian cancer (Mayer et al., 2020). Metagenomic studies have later revealed that the actual producer of trabectedin is a bacterial endosymbiont called *Candidatus Endoecteinascidia frumentensis* (Schofield et al, 2015). The combination of these factors makes sessile marine invertebrates immensely interesting in terms of bioprospecting and discovery of novel compounds.

1.1.4 Bryozoa

Bryozoa (also known as Ectoprocta or Polyzoa) are a phylum of small, aquatic, suspension feeding invertebrates that usually lives in colonies, encased by a hard exoskeleton with pores (Wood, 2015; Campbell et al., 2015). Bryozoan colonies consists of individuals called zooids. Each zooid is made up of the polypide, which includes the soft body parts such as a U-shaped digestive tract and its connected muscular and neural tissue, as well as the cystid, which is the protective body wall. The soft tissue polypide can retract into the protective cystid via retractor muscles. They feed through an organ called the lophophore, which is a collection of ciliated tentacles that is used to scour the surrounding water (Schwaha et al., 2018).

Bryozoans are mainly found in marine environments, except for the class Phylactolaemata, which strictly consists of freshwater species. The class Gymnolaemata also have some species that tolerate brackish water (Koletić et al., 2015). Their habitat ranges from the Arctic depths of the North Sea to the tropical waters of Puerto Rico and Malaysia. Bryozoans can be found in very shallow water (<10 m) as well as in the deep sea, with recorded findings at around 3400 meters depth in the Sea of Okhotsk in the western Pacific Ocean (Grischenko & Chernyshev, 2018; Taylor et al., 2016).

Bryozoan colonies are diverse and can have a variety of structures. Some species have an encrusting colony shape forming a layer around rocks or shells, while others are erect with branch- or treelike structures (Kuklinski, 2009). Common for all bryozoans are their benthic and sessile nature, which makes them unable to escape from potential predators. Due to their

immobility, evolution has granted bryozoans a multitude of other defence mechanisms, represented by a huge variety of secondary metabolites. These include macrocyclic lactones, alkaloids, sterols and sphingolipids with antitumor, antibacterial, inhibitory and cytotoxic effects (Tian et al., 2018). One stellar example is the bryostatins, a group of macrocyclic lactones derived from the marine bryozoan *Bugula neritina*. Bryostatin 1 was first discovered by George Pettit and his colleagues in 1968 and later isolated and characterized (Pettit et al., 1982) (Figure 2). Later studies have revealed numerous bryostatin analogues with promising antineoplastic and cognitive-enhancing properties and are nowadays examined as potential treatments for various types of cancer, Alzheimer's disease, depression and other cognitive conditions (Tian et al., 2018).

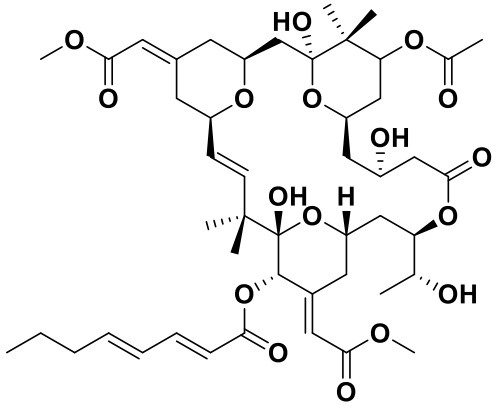

Figure 2 - Molecular structure of Bryostatin 1, isolated from the marine bryozoan Bugula neritina.

1.1.5 Securiflustra securifrons

Securiflustra securifrons is a sessile, temperate and subtidal bryozoan species that belong to the Flustridae family in the Cheilostomata order, which consists of colonies made of a calcium carbonate exoskeleton (Michael et al., 2017; Taylor et al., 2016). Each polypide has the typical bryozoan morphology, including the U-shaped gut and no respiratory or circulatory system. The species is well-distributed in the North Sea and other European coastal waters, as well as abundant in the North Atlantic Ocean (Bock et al, 2020). *S. securifrons* forms erect, branching colonies with an encrusting basal portion that are attached to hard substrates such as rocks or shells.

The Flustridae family is known as a primary source of polycyclic indole alkaloids, mainly from four species; *Chartella papyracea*, *Securiflustra securifrons*, *Hincksinoflustra denticulate* and *Flustra foliacea* (Tian et al., 2017). The earliest discovery of polycyclic indole alkaloids from marine bryozoans, named chartellines A-C and chartellamides A-B, were isolated from *C. papyracea* in the Roscoff region of France in the 1980s (Chevolot et al., 1985; Anthoni et al., 1987). Later, novel halogenated indole-imidazole alkaloids, Securamine A-G and Securine A and B, have been identified from *S. securifrons* off the Danish west coast in the North Sea (Rahbæk et al., 1996; Rahbæk & Christophersen, 1997). Other brominated alkaloids such as flustramines and deformylflustrabromine from *F. foliacea* have been discovered in samples from the North Sea and in Canadian waters, with some exhibiting cytotoxic, antibacterial and antifungal properties (Lysek et al., 2002; Rochfort et al., 2009). Many of these compounds are structurally similar and provide some examples of novel compounds discovered from *S. securifrons* and other species of the Flustridae family.

1.1.6 Securidine A

Securidine A (chemical structure in Figure 3) is a mono-brominated alkaloid that has been isolated from the aqueous extract of *Securiflustra securifrons* (Michael et al., 2017). The structure of Securidine A was novel at the time of isolation. Securidine A is chemically distinguished from other alkaloids isolated from the Flustridae family, such as chartellines and securamines. Securidine A is a brominated tyrosine derivative and structurally related to Pulmonarin B and Synoxazolidinone B, two other brominated tyrosine derivatives isolated from the sub-Arctic ascidian *Synoicum pulmonaria* (Tadesse et al, 2010; Tadesse et al., 2014).

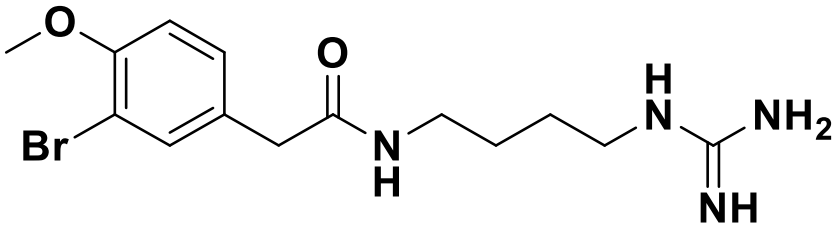

Figure 3 - Molecular structure of Securidine A, isolated from Securiflustra securifrons.

So far, no significant cytotoxic, antibacterial, antidiabetic or biofilm-inhibiting activity has been linked to Securidine A (Michael et al., 2017). However, fractions from organic extracts of *S. securifrons* have shown cytotoxic effects against the human melanoma cell line A2058, most likely associated to bioactive securamines (Hansen et al, 2017). Further testing revealed that Securamine C, E, H and I decreased cell viability of multiple cancer cell lines; human melanoma cell line A2028, human colorectal adenocarcinoma cell line HT-29 and breast cancer cell line MCF-7, as well as the diploid normal cell line MRC-5 (Hansen et al., 2017).

1.1.7 Challenges in marine bioprospecting

Accessibility was always the main issue when comparing marine and terrestrial exploration in the earlier days of bioprospecting. We did not have the knowledge about the vast amount of diversity in our deep seas nor the equipment to access and research it thoroughly. Biological samples from terrestrial habitats were simply more attainable and thus a convenient and logical place to commence the genesis of the bioprospecting era. Nowadays, technological advancements have significantly diminished this barrier with access to precise GPS-systems, underwater robot and camera technology, scuba diving, collection techniques etc. However, there are still issues regarding the amount of resources and time it takes to plan and execute field trips, as well as the collection and preservation of marine samples during expeditions. Biomass samples have limited yield and there is no guarantee that the requested specimen will be found at the same location time after time. This is known as the “supply problem”, which can be a huge obstacle for the commercialization of products, where the principle of supply and demand is essential. Since bioactive secondary metabolites often are species-specific, the

access to a stable supply can become a huge concern. Recollection from natural habitats are often complicated due to seasonal changes and sustainability, as well as environmental, ecological, legal and ethical considerations (Atanasov et al., 2015; Rose et al., 2012). Other possible solutions to the supply problem are aquaculture, semi-synthetization or microbial engineering, all with their particular difficulties and advantages. Progress in the field of synthetic and microbial approaches are continuously being made and obtaining a sustainable supply through synthetic methods is the common solution for marine natural products (Hunt & Vincent, 2006).

Challenges concerning dereplication is another well-known issue, but also an essential process which is used for rapid identification of known compounds to prevent rediscovery and recharacterization (Hubert et al., 2017; Kildgaard et al., 2017). The dereplication process usually involves an untargeted analysis approach (see section 1.2.3), combined with database searches (Hubert et al., 2017). As novel compounds are continuously being discovered, characterized and publicized, the dereplication process becomes increasingly important in line with ever-expanding databases. Quick and effective dereplication will save time, effort and funding so that minimal resources are wasted.

Isolation of compounds from natural samples is often an issue due to their high complexity. High number of components in a sample makes it challenging to isolate target compounds to sufficient purities suitable for NMR and bioactivity analysis. Complex natural extracts are often incompatible with modern high-throughput sequencing methods, since they interfere with assay reagents, decompose or precipitate due to high viscosity and presence of non-specific binding proteins (Atanasov et al., 2015). The structural complexity of secondary metabolites (e.g. the high number of chiral centers) creates many obstacles to overcome, such as optimized hosts for scale-up production and improved computational tools for pathway and host design (Breitling & Takano, 2016).

1.2 Methods in bioprospecting

The bioassay-guided workflow typically conducted at Marbio for invertebrate samples, and also used for this thesis, is illustrated below (Figure 4). Marbio is an analytical platform at the Arctic University of Norway, that performs screening, isolation and identification of bioactive natural products.

The sample collection, extraction, pre-fractionation and initial bioactivity screening was performed prior to the work of this thesis. Collection, species identification, extraction and preservation of samples are initially performed by the Norwegian national marine biobank Marbank, which is co-located with Marbio.

The crude extracts are delivered to Marbio for pre-fractionation and bioactivity screening with various bioassays, including antibacterial, anticancer, anti-inflammatory and biofilm-inhibiting assays (Svenson, 2013). Bioactive crude extracts are subject to further research, continuing with dereplication and subsequent isolation using combined analytical techniques including liquid chromatography (LC) and mass spectrometry (MS). After isolation of a suspected novel compound with sufficient purity and quantity, the sample is sent to nuclear magnetic resonance (NMR) analysis for structure elucidation. The bioprospecting pipeline concludes with bioactivity characterization to pinpoint and expound the bioactive profile of the novel compound.

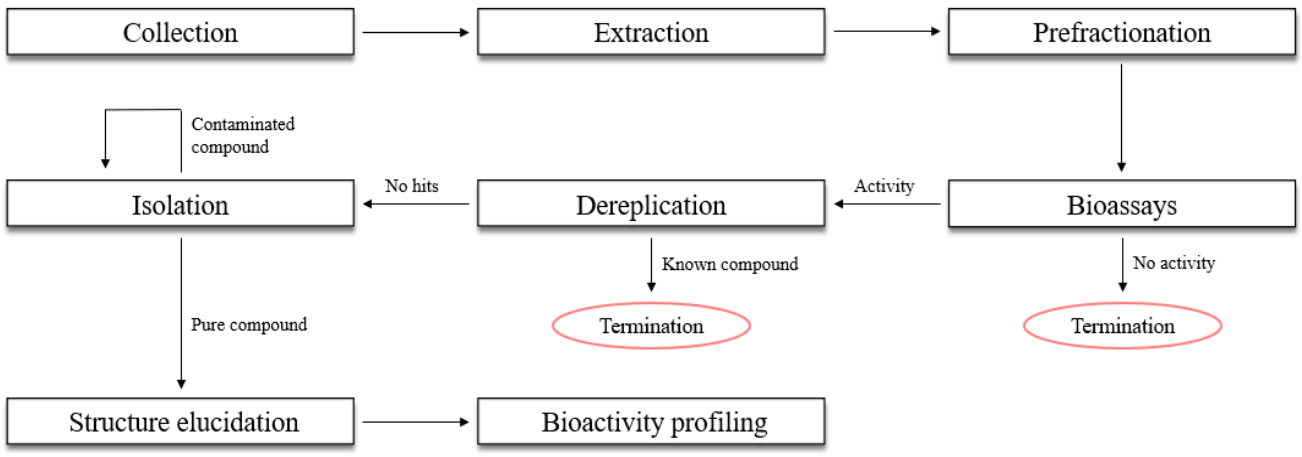

Figure 4 - Overview of the bioassay-guided bioprospecting pipeline used at Marbio.

1.2.1 Sample preparation

Sample preparation is a necessary step in any bioprospecting campaign, as biomass of marine organisms cannot be used directly in bioassays and for compound isolation. The most common method of extraction is liquid-liquid partitioning, where the mixing of two immiscible liquids, usually water (polar) and an organic (non-polar) solvent will separate compounds based on their solubility, resulting in two extracts; aqueous and organic (Berk, 2018). The aqueous extract will contain more polar components, while the organic extract consists of less polar components.

After separation, the extracts are dried under reduced pressure, either by freeze-drying or by a rotavapor or vacuum centrifuge. The prepared extracts can be used to screen for bioactivities and isolate active compounds.

1.2.1.1 Prefractionation

Crude extracts are complex mixtures, often composed of hundreds of different constituents. Prefractionation refers to the fractionation of crude extracts prior to further research, like bioactivity screening and isolation. Pre-fractionation is performed to reduce sample complexity and remove components that can cause "false positives" during bioassays. Components like salts, sugars and lipids possess bioactive properties and can camouflage the bioactivity from secondary metabolites during testing. Prefractionation is not essential for the output of novel compounds but has been shown to increase the hit rate and effectiveness of bioactive screening due to the reduction of interfering compounds (Appleton et al., 2007). Prefractionation can be performed using a variety of different approaches, with chromatographic techniques such as HPLC or flash chromatography being common. Other simpler methods include filtration and solid-phase extraction (Appleton et al., 2007). The number of fractions obtained can vary from few to hundreds, depending on fractionation technique, sample complexity and intended use. At Marbio, flash chromatography resulting in eight fractions is used for prefractionation, where molecules with similar lipophilicity are concentrated into separate fractions (Svenson, 2013).

1.2.2 Bioactivity screening

As part of the bioactivity-guided isolation process, the pre-fractionated crude extracts are submitted to bioactivity screening. This step aims to identify fractions with bioactive components, that can later be isolated and retested. There are numerous different bioassays that can be performed, both *in vivo* and most commonly, *in vitro*, depending on the aim and focus of the research. *In vivo* refers to tests on living organisms, while *in vitro* tests are performed at cell cultures, in petri dishes or test tubes.

At Marbio, a combination of *in vitro* bioassays focused on antimicrobial, anticancer, anti-inflammatory, antidiabetic and biofilm-inhibiting effects are usually performed during the initial screening (Svenson, 2013). The initial screening aims to test a large number of samples in a short amount of time, which is known as high-throughput screening (HTS). Dilution curves of active fraction are created to determine which fractions produce the most promising dose-response results. The most active fractions, that portrays activity at the lowest tested concentrations, are good candidates for further research (Svenson, 2013).

1.2.3 Dereplication

Dereplication refers to the rapid identification of known compounds in crude extracts or fractions (Hubert et al., 2017; Kildgaard et al., 2017). The process intends to increase efficiency and prevent rediscovery and recharacterization, so that resources can be distributed towards novel research. Analytical tools, such as chromatographic and spectroscopic methods have become the favored approach for dereplication purposes. Ultra-high performance liquid chromatography is a specialized chromatographic method of analytical HPLC (see section 1.2.4.1) that provides better resolution, higher speed and lower use of solvent compared to its predecessor (Dong & Zhang, 2014). In analytical HPLC, the goal is to perform analysis of sample composition though column separation and the injected sample is observed by a detector, often coupled with a high resolution mass spectrometer (HR-MS).

HR-MS is extremely sensitive and accurately measures molecular weight by mass-to-charge (*m/z*) ratio of ions. The *m/z*-ratio refers to molecular mass (m) divided by the electrical charge (z). The principle of MS is based upon ionization of molecules by adding electrical charge (H^+) and the analytes are separated according to their *m/z*-ratio (Ho et al., 2003; Pedersen-Bjergaard & Rasmussen, 2004). Since molecules are protonated to form cations, the measured *m/z*-ratio is usually the molecular weight of the separated compound plus the added proton [$M+H^+$]. The most common ionization technique used when analyzing liquid samples is electrospray ionization (ESI). ESI uses electrical energy to ionize molecules directly from the liquid phase to gas phase, making it easily compatible with analytical chromatographic techniques like HPLC. Additionally, ESI maintain low chemical specificity and generate stable ions along with a high ionization efficiency, which has established it as reliable ion source (Wilm, 2011).

The combination of UHPLC and HR-MS makes for a powerful dereplication tool that efficiently separates analytes and produces data in form of isotopic patterns and molecular weight, which can be used to determine the elemental composition and relative abundancy of separated compounds. The elemental composition and exact mass are used to conduct comparative searches throughout numerous databases. Some notable natural products- and chemical-based databases are MARINLIT and ChemSpider. The dereplication process relies upon calculated elemental compositions and available data, thus is not flawless. Regardless, it remains an essential procedure to streamline natural products discovery efforts.

1.2.4 Isolation

Isolation of target compounds is essential in order to accurately elucidate chemical structure and validate bioactive characteristics (Pauli et al., 2012). Purity is key to reduce interference, so the isolation process can often be protracted and strenuous in order to achieve sufficient quantities and purity of target compounds. Isolation can be accomplished using different techniques, depending on the chemical properties, relative abundancy and types of other constituents in the extract.

1.2.4.1 Mass-guided preparative high-performance liquid chromatography

High performance liquid chromatography (HPLC) is an analytical technique that is used to separate analytes according to physiochemical properties, such as molecular weight, polarity, charge or lipophilicity. The setup in an HPLC system can vary depending on the type of chromatography performed, but the principle is to inject the sample into a packed column that acts as a stationary phase, while the analytes are being eluted by pumping through a mobile phase with constant flow and high pressure (Pedersen-Bjergaard & Rasmussen, 2004). The mobile phase usually consists of a solvent mixture, commonly water mixed with acetonitrile or methanol. The solvent composition can be isocratic (constant) or a gradient where the mixture changes during elution. The compounds will be eluted based on their specific affinity to the stationary phase (column) and the mobile phase composition. There are plenty variants of columns available. Choice of column depends on the method of chromatography performed, as well as the contents of the sample. Some of the most common variants of chromatography are reversed-phase, normal-phase, size exclusion and ion exchange (Latif & Sarker, 2012). For reversed-phase chromatography, where the stationary phase is more nonpolar than the mobile phase, the preferred option is often silica-based columns with various degree of silanization and other chemical alterations. Initial column testing and optimization is important to increase efficiency of isolation and purification of target compounds when preforming preparative HPLC.

Preparative (or semi-preparative, when performing on a smaller scale) HPLC is the common variant used to isolate, purify and collect target compounds on a larger scale (Latif & Sarker, 2012). This method utilizes increased flow rate, particle size and injection volume compared to the more sensitive UHPLC to obtain sufficient quantities of the desired compounds. After column separation, a flow splitter will divide the mobile phase to a fraction collector and the detector. Only a small fraction (~1% with a 1/100 splitter) of the sample is observed by the detector, while the remaining sample is collected in fractions triggered by specific target masses or retention time. The detector is commonly based upon ultraviolet-visible (UV-Vis) spectroscopy and measures the absorption of both ultraviolet and visible light at different wavelengths (200-600 nm), which allows for analytes to be identified (Latif & Sarker, 2012; Snyder et al., 1997). HPLC is often coupled with a mass spectrometer (MS), that ionizes

molecules by adding electrical charge (H^+) and separates them according to their mass-to-charge (*m/z*) ratio (see section 1.2.3). The generated output of HPLC-MS analysis includes chromatograms of separated eluents and corresponding mass spectrums which can be analyzed to locate target compounds and adjust fractionation parameters. An example of a coupled HPLC-MS setup is shown in Figure 5.

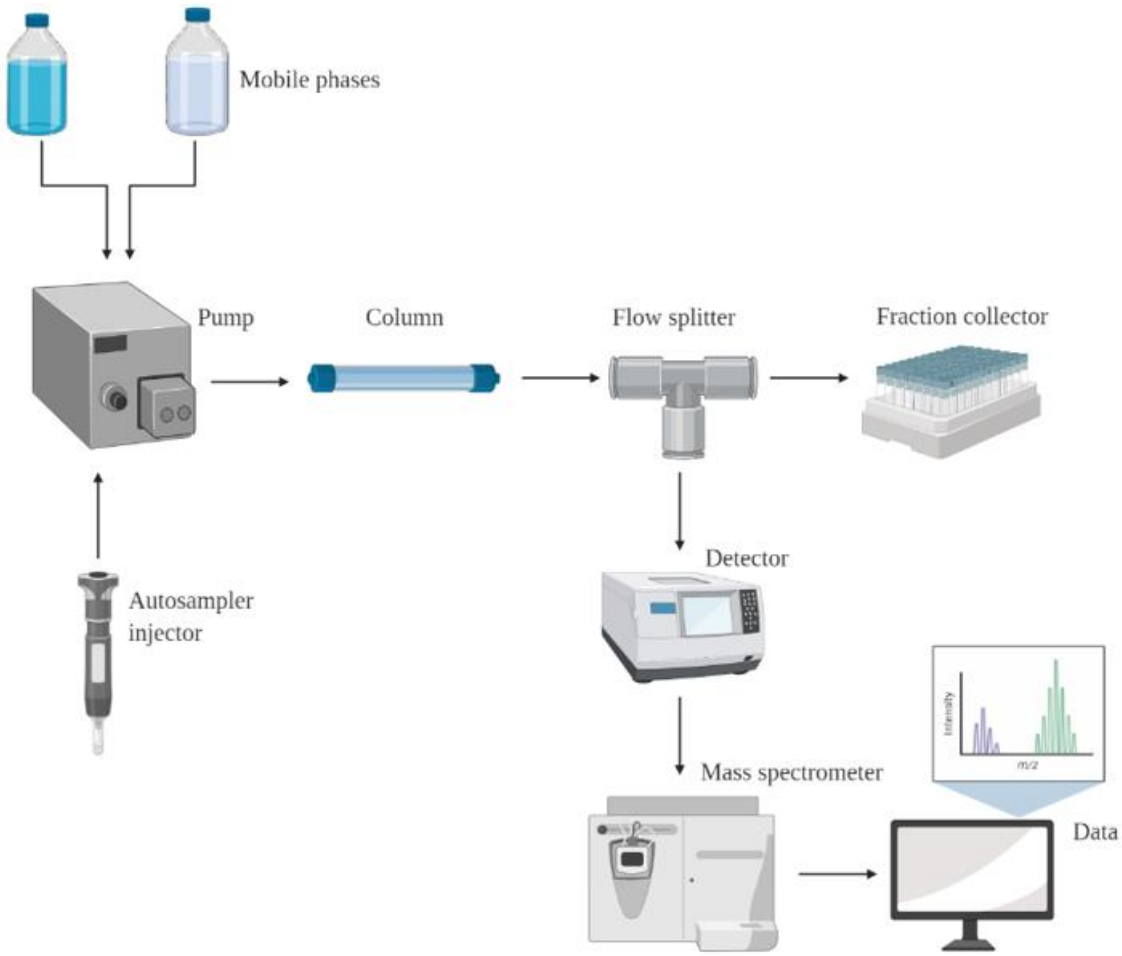

Figure 5 - Simplified overview of a coupled HPLC-MS system. *Made in BioRender.*

1.2.5 Nuclear magnetic resonance (NMR) spectroscopy

Spectroscopy is the study of absorption and emission of electromagnetic radiation by matter. Nuclear magnetic resonance (NMR) spectroscopy is a method frequently used for accurate structure elucidation of organic compounds. This technique is based upon interactions of nuclear spins in magnetic fields and exploits the physical phenomenon where a nucleus in an external magnetic field absorbs and re-emit electromagnetic radiation. Certain atomic nuclei exhibit nuclear spin due to their odd number of nucleic protons and neutrons. When subjected to an external magnetic field, the randomly oriented nuclei will align either with or against the applied magnetic field. This creates two different energy states and thus two different spin states (Figure 6). In NMR spectroscopy, a pulse of electromagnetic radiation that fits the difference between the two energy levels (usually radio frequency) is applied, which causes the nuclei to absorb the electromagnetic energy and flip its spin state. After the electromagnetic pulse, the nuclei will re-emit the absorbed energy and return to its original state. This emitted energy produces a measurable signal, called resonance frequency, which is used to collect physical, chemical and structural information about the molecule (Pauli et al., 2005; Lambert et al., 2019).

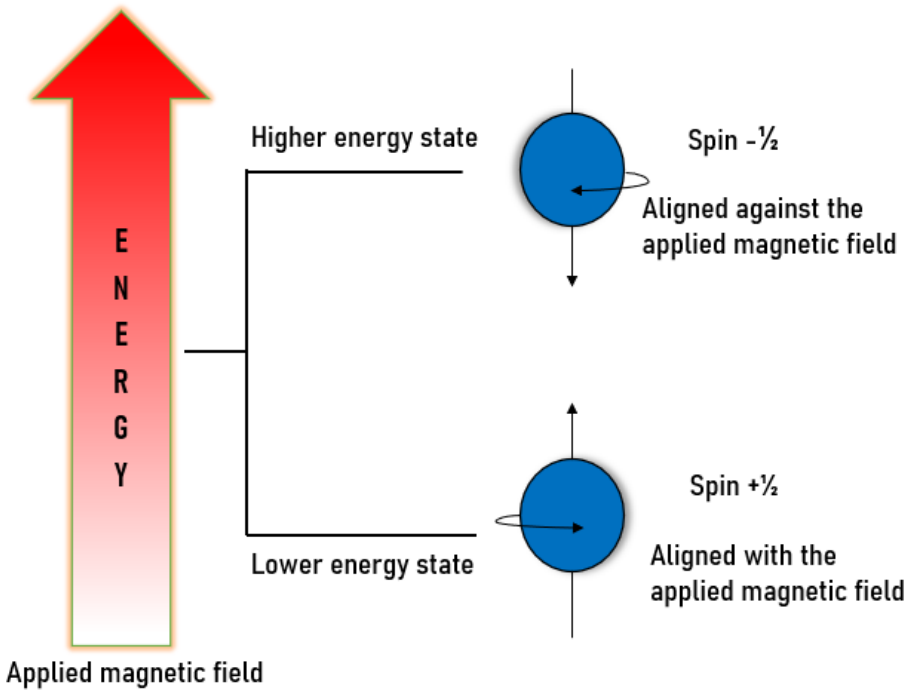

Figure 6 - Energy and spin states of a nuclei in an applied magnetic field.

The obtained information is processed in an NMR spectrum. The two most commonly used isotopes for NMR spectroscopy are ^{1}H and ^{13}C nuclei. ^{1}H-NMR will provide information about chemical shifts and integrations for every hydrogen atom at a different chemical environment in the molecule and ^{13}C likewise about carbon atoms. These are examples of 1-dimensional (1D) experiments, which are analyses of a single nucleus. Two-dimensional (2D) experiments give more precise information about how nuclei are coupled with each other based on a phenomenon known as spin-spin coupling (Pauli et al., 2005). Different 2D experiments are designed to assert different physical information about the given molecule. Some of the most common 2D experiments are correlated spectroscopy (COSY), nuclear Overhauser effect spectroscopy (NOESY), heteronuclear multiple quantum correlation (HMQC) and heteronuclear multiple bond correlation (HMBC). To successfully elucidate complex structures, a combination of several different spectra and analytical data are usually required.

1.2.6 Bioactivity characterization

Isolated compounds will be tested on different bioassays in an attempt to pinpoint any bioactivity. This can be done by testing a wide range of assays for different bioactivities or perform more target-based screening to elucidate possible mode of action for one specific activity. Depending on the knowledge of the compound, individual considerations must be made for optimal utilization of the available isolated amount. This information can include similarity to other known compounds, type of pharmacophore and results from previous testing. The efficiency of bioactive compounds can be determined using quantitative assays such as minimum inhibitory concentration (MIC) or half-maximal inhibitory concentration (IC_{50}).

2 Aim of the thesis

The work performed in this thesis is based upon earlier work conducted at Marbio in 2017, where the novel compound Securidine A was isolated and characterized from the marine bryozoan *Securiflustra securifrons* (Michael et al., 2017). When this isolation was performed, it became evident that the sample contained several halogenated compounds with elemental compositions making it likely that they were structurally related to Securidine A. The compounds were however present is significantly lower amounts compared to Securidine A and was not isolated in sufficient amounts to allow structure elucidation and subsequent bioactivity testing.

In this thesis, the objectives are as follows:

- Identify compounds suspected to be structurally related to the previously reported Securidine A in extracts of the bryozoan *Securiflustra securifrons.*
- Isolate the compounds in amounts sufficient for further analysis. If additional compounds, suspected to be novel structures, are identified in the extract, these will be included in the isolation protocol.
- Determine the structures of the compounds using HR-MS and NMR.
- Determine the bioactivity of the compounds using assays available at Marbio.

3 Materials and methods

A simple overview of the bioprospecting pipeline conducted at Marbio and in this thesis is shown in Figure 3, section 1.2.

3.1 Biological material

The marine bryozoan, *Securiflustra securifrons*, was collected as described in Table 1. The species was identified by the Norwegian National Marine Biobank (Marbank, Institute of Marine Research, Tromsø, Norway) and the samples were stored at -23 °C in the dark until further processing.

Sample M13065 was collected October 2013 off the coast of Rønnebeckøyane, Spitsbergen, Norway using a triangular bottom scrape at 49 m depth. The wet weight of the sample was 2562.11 g.

Sample M19011 was collected April 2019 in Hinlopenstretet between Spitsbergen and Nordaustlandet using a triangular bottom scrape at 76 m depth. The wet weight was 1276.67 g.

Table 1 - Information about collection of biomass samples M13065 and M19011.

Sample	Species	Date	Location	Depth (m)	Wet Weight (g)	Method
M13065	*Securiflustra securifrons*	30.10.2013	Rønnebeckøyane, Spitsbergen, Norway	49	2562.11	Triangular bottom scrape
M19011	*Securiflustra securifrons*	30.04.2019	Hinlopenstretet, Spitsbergen / Nordaustlandet, Norway	76	1276.11	Triangular bottom scrape

3.2 Aqueous sample extraction

Marbio is co-located with Marbank, which routinely prepares extracts from marine invertebrate samples. Both samples were thus available prior to the start of this master project. The equipment and solvents used are listed in Table 2.

Table 2 - Equipment and solvents used for aqueous extraction.

Equipment and solvents	Supplier
Rotary evaporator, Heidolph Laborota	Heidolph, Schwabach, Germany
Centrifuge, Heraeus® Multifuge® 3S-R	Kendro, Osterode, Germany
Milli-Q® Ultrapure water (ddH_2O)	Merck KGaA, Darmstadt, Germany

An overview of the aqueous sample extraction performed at Marbank is shown in Figure 7. Briefly, the aqueous extracts of *S. securifrons* were prepared by initially freezing the biomass. The biomass was then diced and freeze-dried. The dry biomass was ground and extracted twice with double-distilled water (ddH_2O) at 5 °C in darkness. After centrifugation at 4000 rpm at 5 °C for 30 min, the supernatants were collected and dried under reduced pressure at 40 °C. Both extracts were stored at -23 °C until further use.

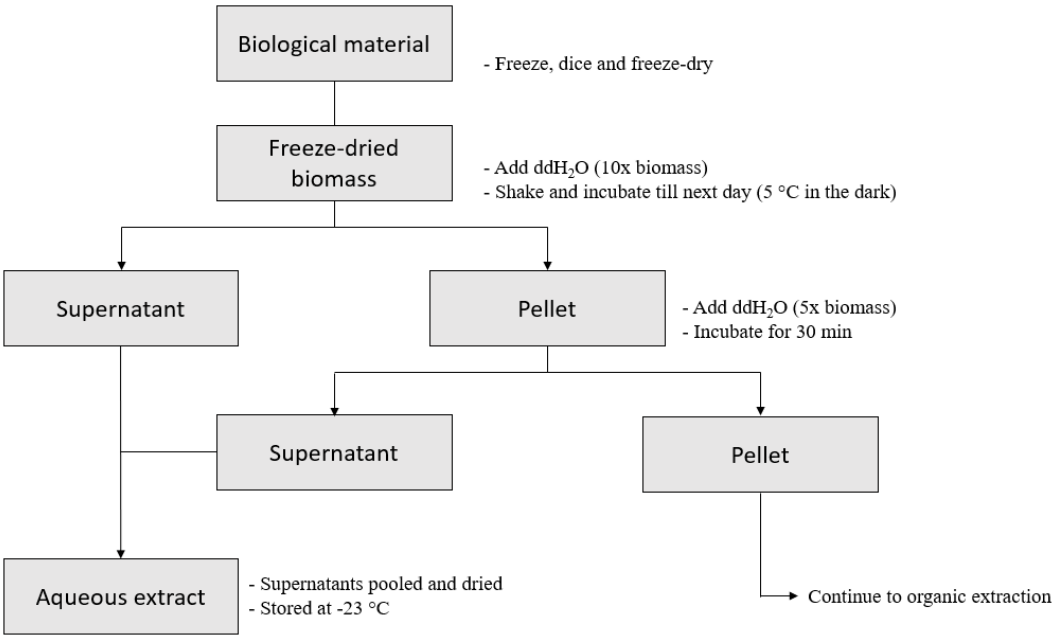

Figure 7 - Preparation of aqueous extracts from marine invertebrates routinely performed by Marbank.

3.3 Preparation of extracts for dereplication and isolation

The aqueous extracts exist as a fibrous powder and needs to be processed prior to further analysis. This was done by methanol (MeOH) extraction. The equipment and solvents used for the extraction are presented in Table 3.

Table 3 - Equipment and solvents used for methanol extraction.

Equipment and solvents	Supplier
Rotary evaporator, Heidolph Laborota	Heidolph, Schwabach, Germany
Centrifuge, Heraeus® Multifuge® 3S-R	Kendro, Osterode, Germany
Methanol (MeOH)	Sigma-Aldrich, MO, USA
Milli-Q® Ultrapure water (ddH_2O)	Merck KGaA, Darmstadt, Germany

The aqueous extract of M13065 (2.0084 g) was resuspended in 100 mL 90% MeOH, and left for 10 min before being centrifuged at 4000 rpm for 5 min. The supernatant was transferred to a round bottom flask and dried using a rotavapor. The sample solvents were removed until the sample volume was approximately 5 mL.

The remaining pellet was suspended in 160 mL 90% MeOH, mixed and left for 5 min before being spun down as earlier. The supernatant was transferred to a new round bottom flask and dried in a rotavapor as described above. This extraction process was repeated once more on the remaining pellet. The nearly dried samples were combined in one round bottom flask, dried until the remaining volume was approximately 7 mL and incubated at 4 °C until analysis.

After target compounds had been isolated and weighted from the M13065 extract (methods described in sections 3.4 - 3.6), the appropriate amount of dry weight needed in order to isolate sufficient amounts of target compounds for NMR analysis was calculated (minimum 1 mg), and the process was repeated with 5.019 g dry weight of extract M19011.

3.4 Dereplication of target compounds

The equipment and solvents used for dereplication with UHPLC-ESI-HR-MS analysis of the aqueous extracts of *S. securifrons* are listed in Table 4.

Table 4 - Equipment and solvents used for UHPLC-ESI-HR-MS analysis of aqueous extracts.

Equipment and solvents	Supplier
Acquity UPLC® C18, 2.1 x 100 mm, 1.7 µM column	Waters, MA, USA
Acquity Sample Manager - FTN	Waters, MA, USA
Acquity Binary Solvent Manager	Waters, MA, USA
Acquity PDA detector	Waters, MA, USA
Vion IMS QTOF	Waters, MA, USA
UNIFI® Scientific Information System	Waters, MA, USA
LiChroSolv® Acetonitrile, hypergrade for LC-MS	Merck KGaA, Darmstadt, Germany
LiChroSolv® Methanol, hypergrade for LC-MS	Merck KGaA, Darmstadt, Germany
LiChroPur® Formic acid 98% - 100%, for LC-MS	Merck KGaA, Darmstadt, Germany
Milli-Q® Ultrapure water (ddH_2O)	Merck KGaA, Darmstadt, Germany

Two samples of the aqueous extracts (M13065 and M19011), previously prepared for chemical analysis by MeOH extraction, were further prepared for UHPLC-ESI-HR-MS by mixing 10 µL of sample with 0.5 mL MeOH in a HPLC vial. The samples were analyzed using a mixed gradient of two mobile phases. Phase A was ddH_2O with 0.1% formic acid (FA), while phase B was acetonitrile (ACN) with 0.1% FA (see Table 5). The injection volume was 7 µL from each sample and the runtime was 15 min with a flow of 0.45 (mL/min). The results were used to locate target compounds and perform dereplication of selected compounds.

Table 5 - Solvent gradient used for UHPLC-ESI-HR-MS analysis on aqueous extracts.

Time (min)	Flow (mL/min)	Mobile phase A (%)	Mobile phase B (%)
Initial	0.45	90	10
12	0.45	10	90
14	0.45	10	90
15	0.45	90	10

To identify potential Securidine A analogues, a thorough analysis of the data was performed using the UNIFI® software from Waters. This was done by manual inspection of sample components from individual peaks, and by utilizing software features that identifies halogenated compounds in the dataset. The elemental composition of compounds with an isotopic pattern with a 1:1 intensity difference between the most intensive peaks, indicating that the compound was mono-brominated, was calculated (Figure 8). To get an initial indication to whether these compounds were structurally related to Securidine A, their calculated elemental compositions were compared to the known structure of Securidine A. In addition, manual searches for masses of likely Securidine A analogues was performed, such as for the debrominated version of Securidine A and the debrominated versions of the identified suspected Securidine A analogues. Fragmentation patterns of the target compounds were also evaluated since it can reveal structural information about the compounds.

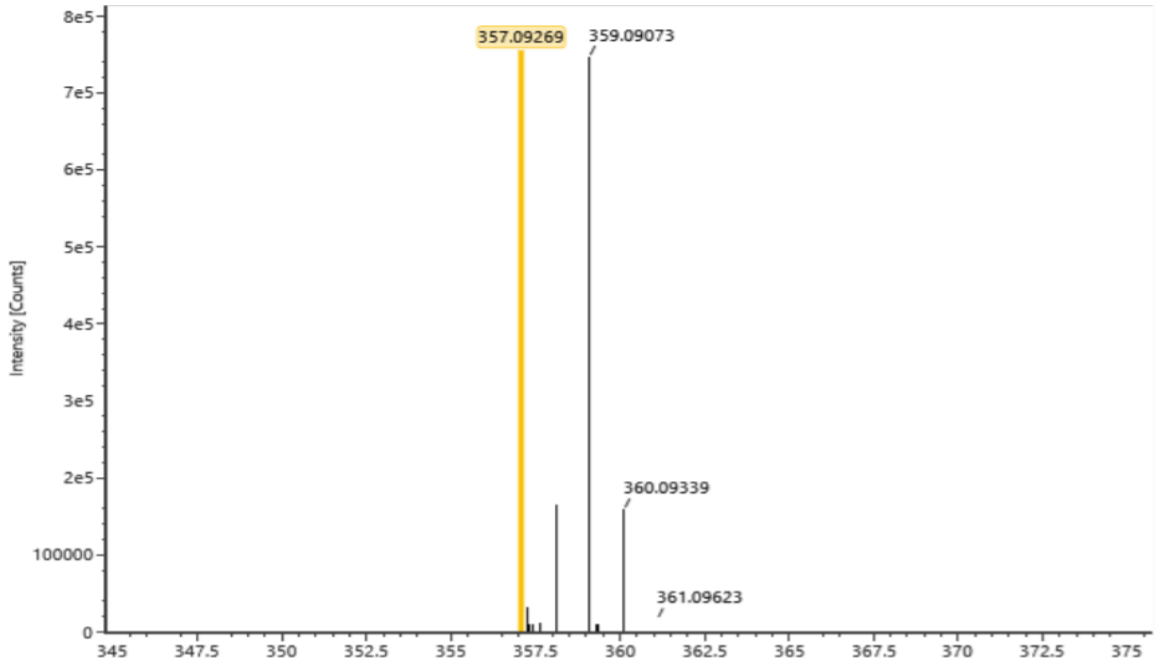

Figure 8 - Example of the isotopic pattern characteristic for mono-brominated compounds. *This example is from Securidine A from extract M13065. 357.09269 represents an elemental composition of $C_{14}H_{22}Br^{79}N_4O_2$, and 359.09073 an elemental composition of $C_{14}H_{22}Br^{81}N_4O_2$. The ^{13}C peaks are also clearly visible.*

To avoid reisolation of already known compounds, dereplication was performed on the target compounds using the calculated elemental composition, neutral mass and fragmentation pattern as input for numerous database searches through UNIFI®.

3.5 Isolation of target compounds

The isolation of target compounds was performed using mass-guided semi-preparative HPLC analysis. First, the most favorable column material for isolation was chosen by executing scouting runs on four different columns. After column selection, the optimal gradient for separation and collection was chosen. Target compounds were collected in separate fractions during each run. Fractions containing the same target compound were pooled, dried and their purity were analyzed to evaluate if further purification was necessary.

3.5.1 Optimization of isolation method

The equipment and solvents used for method optimization and initial purification are listed in Table 6.

Table 6 - Equipment and solvents used for isolation with semi-preparative HPLC of aqueous extracts.

Equipment and solvents	Supplier
Waters 2767 Sample Manager	Waters, MA, USA
Waters 515 HPLC Pump	Waters, MA, USA
Waters 600 Controller	Waters, MA, USA
Waters Prep Degasser	Waters, MA, USA
Waters Flow Splitter (1:100)	Waters, MA, USA
Waters 2996 Photodiode Array Detector	Waters, MA, USA
Waters 3100 Mass Detector	Waters, MA, USA
XSELECT™ CSH™ Prep Fluoro-phenyl 5µM, 10 x 250 mm	Waters, MA, USA
XSELECT™ CSH™ Phenyl-Hexyl Prep 5µM, 10 x 250 mm	Waters, MA, USA
XTerra® Prep MS C8 10 µM, 10 x 250 mm column	Waters, MA, USA
Atlantis® Prep dC18 OBD™ Prep 100Å, 10 µM, 10 x 250 mm	Waters, MA, USA
MassLynx® V4.2 (software)	Waters, MA, USA
PrepSolv® Acetonitrile for preparative chromatography	Merck KGaA, Darmstadt, Germany
Formic acid puriss. pa, ACS reagent, reag. Ph. Eur., >=98%	Sigma-Aldrich, MO, USA
HiPerSolv Chromanorm® Methanol, HPLC gradient grade	VWR, PA, USA
Milli-Q® Ultrapure water (ddH_2O)	Merck KGaA, Darmstadt, Germany

Prior to the isolation, the prepared aqueous extracts (M13065 and M19011) were dissolved in MeOH until the sample's constituents were completely dissolved (approximately 20-25 mL MeOH per extract). Extract M13065 was used for the optimization of the column and the isolation process was performed. Afterwards, extract M19011 was prepared and isolated using the optimized method.

In order to select the best suited column for isolation of target compounds, the diluted M13065 extract was injected onto four columns with different packing materials, a procedure known as a scout run. The four different columns were:

- XSELECT™ CSH™ Prep Fluoro-phenyl, 5 µm, 10 x 250 mm
- XSELECT™ CSH™ Phenyl-Hexyl, 5 µm, 10 x 250 mm
- XTerra® C8, 10 µM, 10 x 250 mm
- Atlantis® dC18, 10 µM, 10 x 250 mm

The runtime was set to 22 min and the injection volume to 300 µL. The gradient used consisted of two mobile phases. Phase A was ddH_2O with 0.1% FA, while phase B was ACN with 0.1% FA (Table 7).

Table 7 - Solvent gradient used for testing and optimization of columns with semi-preparative HPLC of aqueous extracts.

Time (min)	Flow (mL/min)	Mobile phase A (%)	Mobile phase B (%)
Initial	6.00	90	10
15.00	6.00	0	100
20.00	6.00	0	100
20.10	6.00	90	10
22.00	6.00	90	10

The base peak intensity (BPI) chromatograms from each column were analyzed, along with the ion chromatograms of all target compounds. To select the best suited column, several criteria were evaluated. All target compounds must elute as distinct peaks and have proper separation from each other. If these criteria are met by several columns, the column where the target compounds co-elute with the lowest number of impurities is selected. Other minor factors such as pressure on the machinery and runtime length were also considered.

3.5.2 First purification

After initial test runs, the gradient was adjusted to 11 min with a linear slope 10-58% B. The injection volume was increased to 500 µL (Table 8). Phase A was ddH_2O with 0.1% FA, while phase B was ACN with 0.1% FA.

Table 8 - Solvent gradient used for initial purification of target compounds with semi-preparative HPLC.

Time (min)	Flow (mL/min)	Mobile phase A (%)	Mobile phase B (%)
Initial	6.00	90	10
8.00	6.00	42	58
8.10	6.00	0	100
10.00	6.00	0	100
10.10	6.00	90	10
11.00	6.00	90	10

The first purification step was performed using the optimized method. Each target mass was isolated into separate fractions using either automatic mass triggering or timed events according to retention time (RT). Corresponding fractions were pooled in separate round bottom flasks and dried almost completely using a rotavapor. Samples were stored at approximately 4 ℃.

3.5.3 Second purification

The equipment and solvents used for the second purification step are listed in Table 9.

Table 9 - Equipment and solvents used for the second purification process of target compounds.

Equipment and solvents	Supplier
Atlantis® T3 3 µM, 3.0x15 mm C_{18} column	Waters, MA, USA
Acquity Sample Manager - FTN-R	Waters, MA, USA
Acquity Quaternary Solvent Manager	Waters, MA, USA
Acquity Isocratic Solvent Manager	Waters, MA, USA
Acquity QDa detector	Waters, MA, USA
Acquity Fraction Manager	Waters, MA, USA
Waters 2998 Photodiode Array Detector	Waters, MA, USA
Waters Flow Splitter (1:50)	Waters, MA, USA
MassLynx® V4.2 (software)	Waters, MA, USA
LiChroSolv® Acetonitrile, hypergrade for LC-MS	Merck KGaA, Darmstadt, Germany
LiChroSolv® Methanol, hypergrade for LC-MS	Merck KGaA, Darmstadt, Germany
LiChroPur® Formic acid 98% - 100%, for LC-MS	Merck KGaA, Darmstadt, Germany
Dimethyl sulfoxide (DMSO)	VWR, PA, USA
Milli-Q® Ultrapure water (ddH_2O)	Merck KGaA, Darmstadt, Germany

The purity of every isolated compound was examined using UHPLC-ESI-HR-MS (same protocol as section 3.4). Only one sample, containing Securidine A, was pure enough after the initial purification to be directly freeze-dried and stored for further analysis. Another target compound, only known as compound 373, was discarded from further purification due to low yield and purity. The remaining target compounds had to undergo a second purification process. Prior to the second step, the samples were dissolved in a mixture of MeOH and dimethyl sulfoxide (DMSO), adjusted according to the individual sample size and relative solubility (Table 10).

Table 10 - Amounts of MeOH and DMSO used to dissolve samples prior to the second isolation.

Given name	Target mass	MeOH	DMSO
MBC-339	325	4.5 mL	220 µL
MBC-340	343	3 mL	50 µL
MBC-341	367	3.5 mL	50 µL
MBC-342	265	2.5 mL	50 µL

The second purification step was performed on an Acquity Arc system, using a smaller column, reduced flow and lower injection volume. The column temperature was maintained at 40 °C to improve separation. During the process, the method was optimized for each individual target compound through experimentation with various gradients to generate the best possible separation. In each instance, mobile phase A consisted of ddH_2O with 0.1% FA, while mobile phase B consisted of ACN with 0.1% FA.

MBC-339 used a linear gradient 0-40% B for 8 min, completed by washing steps for the last 5 min (Table 11).

Table 11 - Gradient used for target compound MBC-339 during second purification run.

Time (min)	Flow (mL/min)	Mobile phase A (%)	Mobile phase B (%)
Initial	1.00	100	0
8.00	1.00	60	40
8.10	1.00	0	100
11.00	1.00	0	100
11.10	1.00	100	0
13.00	1.00	100	0

MBC-340 used a linear gradient 0-20% B for 15 min with washing steps for the final 6 min (Table 12).

Table 12 - Gradient used for target compound MBC-340 during second purification run.

Time (min)	Flow (mL/min)	Mobile phase A (%)	Mobile phase B (%)
Initial	1.00	100	0
15.00	1.00	80	20
15.10	1.00	0|	100
18.00	1.00	0	100
18.10	1.00	100	0
21.00	1.00	100	0

MBC-341 used 100% A for 2 min, then gradually 0-20% B for 8 min, concluded by washing steps for 6 min (Table 13).

Table 13 - Gradient used for target compound MBC-341 during second purification run.

Time (min)	Flow (mL/min)	Mobile phase A (%)	Mobile phase B (%)
Initial	1.00	100	0
2.00	1.00	100	0
10.00	1.00	80	20
10.10	1.00	0	100
13.00	1.00	0	100
13.10	1.00	100	0
16.00	1.00	100	0

MBC-342 used a gradient of 100% A for 2 min, then gradually 0-10% B for 8 min, followed by washing steps to equilibrate the column for the last 6 min (Table 14).

Table 14 - Gradient used for target compound MBC-342 during second purification run.

Time (min)	Flow (mL/min)	Mobile phase A (%)	Mobile phase B (%)
Initial	1.00	100	0
2.00	1.00	100	0
10.00	1.00	90	10
10.10	1.00	0	100
13.00	1.00	0	100
13.10	1.00	100	0
16.00	1.00	100	0

After isolation was completed, fractions were collected in round bottom flasks, their purity was reanalyzed (same protocol as section 3.4) and dried using a rotavapor.

3.6 Drying of samples

Equipment and solvents used to dry samples of the isolated compounds are listed in Table 15.

Table 15 - Equipment and solvents used for drying of samples.

Equipment and solvents	Supplier
Savant™ SC250EXP SpeedVac® Concentrator	Thermo Fisher Scientific, MA, USA
Savant™ RVT4104 Refrigerated Vapor Trap	Thermo Fisher Scientific, MA, USA
Heto PowerDry® PL9000	Thermo Fisher Scientific, MA, USA
Heto HSC 500 Plus	Thermo Fisher Scientific, MA, USA
Dimethyl sulfoxide (DMSO)	VWR, PA, USA
Methanol (MeOH)	Sigma-Aldrich, MO, USA

The dried samples were dissolved in MeOH and DMSO, adjusted according to their solubility. The dissolved samples were transferred to pre-weighted glass tubes and dried completely in a vacuum centrifuge for 2-5 h. The dried samples were stored at a freezer until frozen if necessary and then freeze-dried using Heto PowerDry® PL9000 for 24-48 h, until completely dry. The freeze-dried samples were weighted and used for further analysis.

3.7 Structure elucidation of novel compounds

Structure elucidation of the novel isolated compounds were attempted with nuclear magnetic resonance (NMR) and by analyzing fragmentation patterns using mass spectrometry (MS). Three of the isolated novel compounds (MBC-339, MBC-340 and MBC-341) were attempted elucidated with NMR, while the structure of MBC-342 was elucidated by fragmentation patterns.

3.7.1 Nuclear magnetic resonance (NMR)

The nuclear magnetic resonance was performed by Johan Isaksson at the Department of Chemistry at UiT - The Arctic University of Norway. The data was interpreted by my supervisor Kine Østnes Hansen at Marbio. The NMR experiments were acquired on a Bruker Avance III HD spectrometer operating at 599.90 MHz for protons, equipped with an inverse detected cryo-probe enhanced for ^{1}H, ^{13}C, and ^{2}H. The NMR samples were prepared in d_6-DMSO. Experiments were typically acquired using gradient selected adiabatic versions where applicable. All experiments were acquired using Top Spin 3.5 pl2 at 298 K.

3.7.2 Fragmentation patterns

MBC-342 was elucidated by observing and analyzing fragments in ESI ± HR-MS (equipment shown in Table 4). The collision conditions were set to 20-60 electron volt (eV) ramp collision energy in order to obtain the first set of fragments (Appendix Figure A1). A second spectra was obtained at a set collision energy of 80 eV with a mass window for the precursor ions set to *m/z* 264-266 in order to suppress noise and ensure proper assignment of fragments (Appendix Figure A2). Dinitrogen (N_2) was used as collision gas for both experiments. UNIFI® was used to calculate the elemental compositions of the obtained fragments.

3.8 Bioactivity testing

In an attempt to elucidate the bioactivities of the five isolated compounds (Securidine A, MBC-339, MBC-340, MBC-341 and MBC-342), the samples were tested in various bioassays. All compounds were tested at 50 µM in three technical replicates for cytotoxic properties against two human cell lines (one malignant and one non-malignant), for antibacterial properties against five bacterial strains (both gram-positive and gram-negative) and for inhibitory effects against both the PTP1B enzyme and biofilm formation. During this initial screening, compound MBC-340 showed activity against one of the cancer cell lines. The IC_{50} value of the compound against this cell line was therefore determined by assaying it in a dilution series.

3.8.1 Preparation of samples

Prior to the bioassays, stock solutions were prepared by dissolving each compound in DMSO to a concentration of 10 μg/μL. The stock solutions were stored at 4 °C and used to dilute the samples to the desired concentration for each bioassay.

3.8.2 Cell proliferation assays

The *in vitro* antiproliferative activities of the five compounds were evaluated against two human cell lines: the malignant melanoma cell line A2058, and the non-malignant lung fibroblast cell line MRC-5. To quantify the antiproliferative activities, a 3-(4,5-dimethylthiazol-2-yl)-5-(3-carboxymethoxyphenyl)-2-(4-sulfophenyl)-2H-tetrazolium (MTS) assay setup was used. Equipment, solvents and biological material used in cell proliferation assays are listed in Table 16.

Table 16 - Equipment, solvents and biological material used in cell proliferation assays.

Equipment, solvents and biological material	Supplier
Sanyo MCO-18AIC CO_2 Incubator	Panasonic Biomedical, Japan
Herasafe™ KS Class II, Type A2 Biological Safety Cabinet	Thermo Fisher Scientific, MA, USA
DTX 880 Multimode detector	Beckman Coulter, CA, USA
Nunc™ Microwell™ 96-well microtiter plate	Thermo Fisher Scientific, MA, USA
Gibco Dulbecco's Modified Eagle Medium (D-MEM)	Thermo Fisher Scientific, MA, USA
Minimum Essentials Medium Eagle (MEM)	Biochrom, Cambridge, UK
Fetal bovine serum (FBS)	Merck KGaA, Germany
Gentamycin (10 mg/mL)	Merck KGaA, Germany
Stable Glutamine (200 mM)	Merck KGaA, Germany
Non-essential amino acids	Biochrom, Cambridge, UK
Sodium pyruvate (100 mM)	Biochrom, Cambridge, UK
Sodium bicarbonate (7.5 %)	Biochrom, Cambridge, UK
Dimethyl sulfoxide (DMSO)	VWR, PA, USA
Phosphate-buffer saline (PBS)	Produced in-house
Trypsin	Thermo Fisher Scientific, MA, USA
Trypan blue	Sigma-Aldrich, MO, USA
Bürker counting chamber	Thermo Fisher Scientific, MA, USA
CellTiter 96® AQueous One Solution Reagent	Promega, WI, USA
A2058 (ATCC® CRL-1147™)	LGC Standards, London, UK
MRC-5 (ATCC® CCL-171™)	LGC Standards, London, UK

Both cell lines were incubated at 37 °C with 5% CO_2. A2058 was cultured and assayed in D-MEM supplemented with 10% FBS, 10 µg/mL gentamycin and 200 mM glutamine stable. MRC-5 was cultured and assayed in MEM supplemented with 10% FBS, 10 µg/mL gentamycin, 200 mM glutamine stable, 5 mL non-essential amino acids, 1 mM sodium pyruvate and 0.15% (w/v) sodium bicarbonate.

To maintain the cells in culture and seed cells into assay plates, the following procedure was performed for both cell lines. The growth medium was removed, and the cells were washed with 10 mL PBS before addition of 2 mL of trypsin. The cells were incubated at 37 °C for approximately 2 min to detach the cells from the flask. The cells were resuspended in 10 mL fresh and preheated growth medium. A new passage of cells was maintained by transferring 1 mL to a new cell growth flask containing 10 mL fresh growth medium.

From the cell suspension, 100 µL was added to an Eppendorf tube with 100 µL trypan blue and mixed. An aliquot of the trypan blue mixture (10 µL) was added to a Bürker counting chamber and the number of cells were counted in a microscope. The volume of cell suspension needed to obtain the desired cell density (2000 cells/well for A2058 and 4000 cells/well for MRC-5) was calculated and then added to fresh growth medium for a total volume of 15 mL. For each well in a 96-well microtiter plate, 100 µL of the cell suspension was added. The plate was incubated at 37 °C with 5% CO_2 overnight to allow cells to adhere to the microtiter plate.

The following day, the growth medium was removed from the cells and the test samples were added in replicates of 50 µL sample + 50 µL growth medium. Four wells containing 90 µL growth medium and 10 µL DMSO were established as positive controls. The remaining wells were added a total of 100 µL growth medium and used as negative controls. The microtiter plates were incubated at 37 °C with 5% CO_2 for 72 h. Subsequently, 10 µL of CellTiter 96® AQueous One Solution Reagent was added to each well and the plates were incubated for 1 h at 37 °C. The absorbance was measured at 485 nm with a DTX 880 multimode detector. Percent cell survival was calculated using the equation below (equation 1). The data was visualized using GraphPad Prism 8.4.2 and IC_{50} was calculated. The built-in ROUT method was used to detect and remove outliers from the dataset (Q = 1%).

Equation 1

$$\%\ cell\ survival: \frac{(absorbance\ treated\ wells - absorbance\ positive\ control)}{(absorbance\ negative\ control - absorbance\ positive\ control)}\ x\ 100$$

The assay against A2058 was repeated with ten dilution steps from 150 µM to 1.56 µM of MBC-340 to calculate the IC_{50} (concentration that inhibits 50% growth). This was done based on the results from the initial assay.

3.8.3 Antifungal assay

The pathogenic yeast *Candida albicans*, which is a common cause for fungal infections, was used to test the antifungal properties of the isolated compounds. Equipment, solvents and biological material used in antifungal assay against *C. albicans* are listed in Table 17.

Table 17 - Equipment, solvents and biological material used in antifungal assay against C. albicans.

Equipment, solvents and biological material	Supplier
Nunc™ Microwell™ 96-well microtiter plate	Thermo Fisher Scientific, MA, USA
Victor Multilabel Plate Reader	PerkinElmer, MA, USA
Gibco Roswell Park Memorial Institute (RPMI) 1640 Medium	Sigma-Aldrich, MO, USA
3-(*N*-morpholino)propanesulfonic acid (MOPS)	Sigma-Aldrich, MO, USA
L-Glutamine	Sigma-Aldrich, MO, USA
Remel 0.5 McFarland Equivalence Turbidity Standard	Thermo Fisher Scientific, MA, USA
Amphotericin B	Sigma-Aldrich, MO, USA
Potato dextrose broth (PDB)	Sigma-Aldrich, MO, USA
Agar-agar	Sigma-Aldrich, MO, USA
Sodium chloride (NaCl)	Sigma-Aldrich, MO, USA
Milli-Q® Ultrapure water (ddH_2O)	Merck KGaA, Darmstadt, Germany
Candida albicans ATCC 90028	LGC Standards, London, UK

Three types of medium were prepared prior to testing. Assay medium consisting of 10.4 g of RPMI powder and 35.53 mg of MOPS buffer was added in 900 mL ddH_2O. The pH was adjusted to 7 and ddH_2O up to 1 L was added. The medium was autoclaved before adding 10.25 mL sterile L-glutamine. Salt medium of 0.9% NaCl was prepared by adding 9 g of NaCl into 1 L ddH_2O. For the potato dextrose agar (PDA), 24 g of PDB and 15 g agar was added into 1 L ddH_2O. The mix was autoclaved and distributed in agar plates.

C. albicans was transferred from freeze stock to new PDA plates and incubated over night at 37 °C. The next day, a few colonies of the culture were resuspended in 0.9% NaCl. The cell density was evaluated using 0.5 McFarland Standard and then adjusted to 1-5 x 10^6 cells/mL by adding more 0.9% NaCl. The yeast suspension was diluted 1:50 and further 1:20 (1-5 x 10^3 CFU/mL) in assay medium.

The samples, controls and yeast suspension were added to the 96-well microtiter plate accordingly (100 µL sample/control + 100 µL yeast suspension). The final concentration of yeast cells was now 0.5-2.5 x 10^3 CFU/mL. Amphotericin B with final concentration of 8 µg/mL was used as the positive control, while autoclaved ddH_2O and growth medium was used as the negative control. The growth control consisted of 100 µL assay medium and 100 µL yeast suspension. The absorbance was measured at 600 nm using a Victor plate reader before the plates were incubated for 48 h at 37 °C. The absorbance was measured again after 48 h.

3.8.4 Antibacterial assay

Five human pathogenic bacterial strains (*E. faecalis*, *E. coli*, *P. aeruginosa*, *S. aureus* and *S. agalactiae*) were used to test the antibacterial growth inhibition of the isolated compounds. Equipment, solvents and biological material used in antibacterial assays are listed in Table 18.

Table 18 - Equipment, solvents and biological material used in antibacterial assays against five bacterial strains.

Equipment, solvents and biological material	Supplier
Nunc™ Microwell™ 96-well microtiter plate	Thermo Fisher Scientific, MA, USA
Victor Multilabel Plate Reader	PerkinElmer, MA, USA
Difco™ Mueller-Hinton (MH) broth	BD Biosciences, CA, USA
Brain heart infusion (BHI)	Sigma-Aldrich, MO, USA
Blood agar plates	UNN, Tromsø, Norway
Gentamycin	VWR, PA, USA
Milli-Q® Ultrapure water (ddH_2O)	Merck KGaA, Darmstadt, Germany
Enterococcus faecalis ATCC 29212	LGC Standards, London, UK
Pseudomonas aeruginosa ATCC 27853	LGC Standards, London, UK
Escherichia coli ATCC 25922	LGC Standards, London, UK
Staphylococcus aureus ATCC 25923	LGC Standards, London, UK
Streptococcus agalactiae ATCC 12386	LGC Standards, London, UK

The bacterial strains were stored in a biofreezer at -80 °C. All strains were streaked onto separate blood agar plates and incubated at 37 °C overnight. A scoop of pathogens from the blood agar plate were transferred to 8 mL of preferred growth media according to Table 19. The cultures were incubated at 37 °C for around 20 h.

Table 19 - Preferred growth medium and number of colony forming units (CFU) for each bacteria used in the antibacterial assay.

Bacteria	Preferred growth medium	Colony forming units (CFU)
E. faecalis	BHI	0.5-3 x 10^5 CFU/mL
E. coli	MH	0.5-3 x 10^5 CFU/mL
P. aeruginosa	MH	3-7 x 10^4 CFU/mL
S. aureus	MH	0.5-3 x 10^5 CFU/mL
S. agalactiae	BHI	0.5-3 x 10^5 CFU/mL

From the bacterial culture, 2 mL of each pathogen were transferred to separate flasks containing 25 mL of preferred growth media (Table 19). The diluted bacterial cultures were incubated for 1.5 h for *E. faecalis*, *E. coli* and *S. agalactiae* and 2.5 h for *P. aeruginosa* and *S. aureus* at 37 °C with 100 rpm. After incubation, the bacterial suspensions were first diluted 1:100 and then 1:10 in growth medium to get the desired CFU-value.

For each well in a microtiter plate, except for the controls, 50 µL of sample replicates and 50 µL of bacterial suspension were added. The medium control consisted of 50 µL medium + 50 µL ddH_2O, and the growth control of 50 µL bacterial suspension + 50 µL ddH_2O. A titration series of gentamycin (0.01 - 16 µg/mL) was used as assay control. The microtiter plates were incubated at 37 °C overnight before the absorbance was measured at 600 nm using a Victor plate reader.

3.8.5 Antibiofilm formation assay

The inhibitory effect on biofilm formation of the isolated compounds was tested on *Staphylococcus epidermis*. The non-biofilm forming bacteria *Staphylococcus haemolyticus* was used as a control. Equipment, solvents and biological material used in antibiofilm formation assay are listed in Table 20.

Table 20 - Equipment, solvents and biological material used in antibiofilm formation.

Equipment, solvents and biological material	Supplier
Nunc™ Microwell™ 96-well microtiter plate	Thermo Fisher Scientific, MA, USA
Victor Multilabel Plate Reader	PerkinElmer, MA, USA
Glucose	Sigma-Aldrich, MO, USA
96% ethanol	UiT, Tromsø, Norway
Crystal violet solution, 1%	Merck KGaA, Darmstadt, Germany
Tryptic soy broth	Merck KGaA, Darmstadt, Germany
Blood agar plates	UNN, Tromsø, Norway
Milli-Q® Ultrapure water (ddH_2O)	Merck KGaA, Darmstadt, Germany
Staphylococcus epidermis (RP62A 42-77)	LGC Standards, London, UK
Staphylococcus haemolyticus	UiT, Tromsø, Norway

A few colonies of *S. epidermis* and *S. haemolyticus* stored on blood agar plates (streaked as described in 3.8.4) was transferred to 5 mL of tryptic soy broth and incubated at 37 °C for approximately 20 h. From the overnight cultures, both bacteria were diluted 1:100 in growth medium with 1% added glucose.

The samples were added in triplicates on a 96-well microtiter plate with 50 µL sample + 50 µL diluted bacterial suspension of *S. epidermis.* The growth control was 50 µL bacterial suspension of *S. epidermis* + 50 µL ddH_2O, while 50 µL bacterial suspension of *S. haemolyticus* + 50 µL ddH_2O is used as a non-biofilm forming control. The medium control consisted of 50 µL growth medium + 50 µL ddH_2O. The microtiter plate was incubated at 37 °C over night and the absorbance measured at 450 nm with a Victor plate reader.

3.8.6 PTP1B inhibition assay

The antidiabetic effect of the isolated compound was tested against the enzyme protein tyrosine phosphatase 1B (PTP1B) which is associated with development of type 2 diabetes. Equipment, solvents and biological material used in PTP1B inhibition assay are listed in Table 21.

Table 21 - Equipment, solvents and biological material used in PTP1B inhibition assay.

Equipment, solvents and biological material	Supplier
Nunc™ black polystyrene 96-well MicroWell™ plate	Thermo Fisher Scientific, MA, USA
DTX 880 Multimode detector	Beckman Coulter, CA, USA
4-(2-hydroxyethyl)-1-piperazineethanesulfonic acid (HEPES)	Sigma-Aldrich, MO, USA
Sodium Chloride (NaCl)	Sigma-Aldrich, MO, USA
Dithiothreitol	Sigma-Aldrich, MO, USA
Ethylenediaminetetraacetic acid (EDTA)	Sigma-Aldrich, MO, USA
Bovine serum albumin (BSA)	Sigma-Aldrich, MO, USA
Protein tyrosine phosphatase 1B (PTP1B)	Sigma-Aldrich, MO, USA
Protein tyrosine phosphatase inhibitor IV (PTP inhibitor IV)	Sigma-Aldrich, MO, USA
6,8-difluoro-4-methylumbelliferyl phosphate (DiFMUP)	Thermo Fisher Scientific, MA, USA
Dimethyl sulfoxide (DMSO)	Sigma-Aldrich, MO, USA
Milli-Q® Ultrapure water (ddH_2O)	Merck KGaA, Darmstadt, Germany

The assay buffer consisted of 25 mM HEPES, 50 mM NaCl, 2 mM dithiothreitol, 2.5 mM EDTA and 0.01 mg/mL BSA. All solvents were dissolved to desired concentration in 500 mL ddH_2O and the pH was adjusted to 7.2. The stock solution was used to dilute PTP1B to a concentration of 31,2 ng/mL, DiFMUP 10 µM and PTP inhibitor IV to 160 µM.

To a black polystyrene microtiter plate, 25 µL of sample, inhibitor or buffer was added to assigned wells. PTP1B (50 µL) was added to every well and the plate was incubated at 37 °C for 30 min. After incubation, 25 µL DiFMUP was added to all wells and the plate was incubated at 37 °C for 10 min. The fluorescence was measured at excitation 360 nm and emission 465 nm using a DTM 880 Multimode detector.

4 Results and discussion

Two aqueous extracts from *S. securifrons* were prepared for analysis and isolation. Dereplication using UHPLC-ESI-HR-MS was performed to identify compounds with elemental compositions indicating structural similarity to Securidine A, confirm the presence of Securidine A and reduce the risk of rediscovery. Isolation of target compounds were completed using semi-preparative HPLC and suspected novel compounds of adequate yield and purity were sent to NMR for structure elucidation. Bioactivity characterization of the suspected novel compounds and Securidine A was performed.

4.1 Motivation behind the work

Securidine A has previously been isolated from an aqueous extract of *S. securifrons* and tested for bioactivity at Marbio, but no bioactivity has been confirmed (Michael et al., 2017). Since it is broadly accepted that natural products are produced to increase the viability of the producing organism, it is highly likely that Securidine A possess bioactive properties that remains to be discovered. The previously isolated amount was consumed during initial efforts and reisolation was therefore necessary before further testing. Securidine A has not been tested against e.g. human pathogenic fungi and kinases known to be upregulated in certain types of cancer or other diseases.

During the previous isolation of Securidine A, several brominated compounds with elemental compositions suggesting a structural similarity to Securidine A was observed. These compounds were present in miniscule amounts and could not be isolated in sufficient quantities. The presence of Securidine A analogues is advantageous for a couple of reasons. Firstly, it indicates that Securidine A and its analogues exhibit some important biological effect(s) since its production seems prioritized in *S. securifrons*. Secondly, having Securidine A analogues readily available is hugely beneficial for further work if the bioactivity of Securidine A is discovered. Natural products usually require chemical optimization in order to become commercially available pharmaceuticals. Testing of the analogues in similar bioactivity assays, and observing differences in potency, will provide an indication regarding the pharmacophore

of the compound group. Such information could aid in future medicinal chemistry campaigns aiming to increase potency and provide insights to how toxicological and pharmacokinetic properties can be improved. It is also possible that Securidine A is inactive in available bioactivity assays, but that some of the analogues show activity. Previously, the staff at Marbio have observed discrepancies in the bioactivity of compounds with the same chemical scaffold, with only minor structural modifications separating them. This was the case for e. g. the Breitfussin family of compounds. Breitfussin A was inactive as a kinase inhibitor, whereas its deiodated analogue, Breitfussin D, displayed a broad kinase inhibitory profile (Hansen et al., 2019).

4.2 Sample preparation

Two aqueous extracts (M13065 and M19011) from the marine bryozoan *S. securifrons* were prepared for further analysis by MeOH-extraction. A total of 2.0084 g dry weight of extract M13065 resulted in approximately 7 mL of prepared sample, while 5.019 g dry weight of extract M19011 resulted in roughly 15 mL of prepared sample. Parts of both aqueous extracts are still available, thus additional amounts of the isolated compounds can be prepared if needed for further research.

4.3 Selection and dereplication of securidine-related compounds

Two aqueous extracts (M13065 and M19011) from the marine bryozoan *S. securifrons* were analyzed using UHPLC-ESI-HR-MS and the subsequent data was used to locate possible analogues of Securidine A, alongside other suitable target compounds. This process would additionally validate the presence of Securidine A and reduce the risk of rediscovery of known compounds. The calculated elemental composition, fragmentation patterns and recorded neutral mass of target compounds were used as inputs for searches through numerous databases already available as an integrated part of the UNIFI® software.

The chromatograms and mass spectrum data from the initial dereplication analysis of the prepared extracts were used to identify possible analogues of Securidine A. This was done by analyzing chromatographic peaks and their corresponding mass spectrums to locate mono-brominated compounds that could potentially be similar to Securidine A. Using a halogen filter in the UNIFI® processing software, several halogenated compounds (25+) were determined to be present in the extracts. Many could easily be determined as structurally unrelated to Securidine A, as dereplication established them to be already known compounds. For instance, several previously reported securamines, including securamine H and C, were identified. As these compounds are well described in literature and already known to not be structurally related to Securidine A (Rahbæk et al., 1996, Hansen et al., 2017), they were not interesting to pursuit further as part of this thesis. Some halogenated compounds were also identified in miniscule quantities, rendering them difficult and time-consuming to isolate in sufficient quantities for NMR analysis. No compounds containing halogens other than bromine were discovered in the extracts.

Five target compounds, four of which were mono-brominated, were chosen for isolation from extract M13065. The same target compounds were chosen from extract M19011, except for compound 373 that was discarded due to low yield and purity. Another non-brominated compound, MBC-342, was added from this extract. A total of six target compounds were initially attempted isolated from the aqueous extracts using semi-preparative HPLC (Table 22). The compounds were given names with the abbreviation MBC-XXX, which is the standard temporary name for novel compounds at Marbio.

Table 22 - Table of compounds isolated from aqueous extracts M13065 and M1901. *Table includes given name, mass (equal to m/z), retention time (RT) and probable mono-bromination status.*

Given name	Mass $[M+H]^+$	RT	M13065	M19011	Brom
Securidine A	357.30	6.2	+	+	+
MBC-339	325.28	6.9	+	+	+
MBC-340	343.21	5.2	+	+	+
MBC-341	367.32	3.5	+	+	-
MBC-342	265.32	1.7	-	+	-
Compound 373	373.35	5.6	+	-	+

The presence of Securidine A was confirmed in both extracts during the dereplication process. Its structure was validated by using its exact mass, elemental composition and fragmentation pattern as inputs in database searches, which yielded a hit in the chemical structure database ChemSpider. Analysis of an available Securidine A sample, whose structure has previously been determined using NMR, was also analyzed as a reference.

Within the preliminary list of halogenated compounds, some were found to have elemental compositions making them probable Securidine A analogues. When comparing their elemental compositions to that of Securidine A, the differences could in some instances easily be explained by applying theory regarding natural product chemistry. Based on these comparisons, probable structures of the target compounds were established. It is likely that securidine variants will have the same chemical backbone as Securidine A since they most likely are produced by the same biosynthetic pathway. The variants will therefore have modified side groups as opposed to differences in the core chemical scaffold. This is proven to be the case for several families of natural products, including bryostatins (Pejin et al., 2014), securamines (Hansen et al., 2017) and orthoscuticellines (Kleks et al., 2020) that are all isolated from bryozoans.

MBC-340 had an unprotonated calculated elemental composition of $C_{13}H_{19}BrN_4O_2$ and is believed to be an analogue of Securidine A where the methoxy group on the benzene ring is exchanged for a hydroxy group (Figure 9). This structure maintains the core chemical scaffold from Securidine A and rationally justifies the difference observed in elemental compositions.

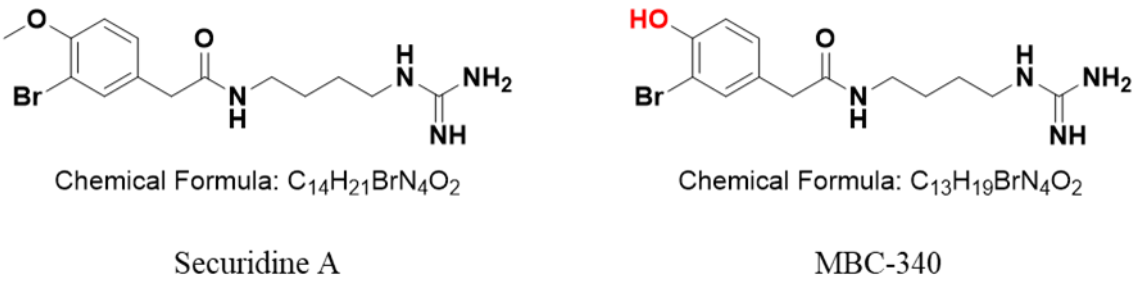

Figure 9 - Proposed structure of MBC-340 made by comparing the elemental composition of the compound to that of Securidine A.

The same comparison of elemental composition was made for other compounds determined to resemble Securidine A. This included MBC-339 and compound 373. MBC-339 ($C_{14}H_{17}BrN_2O_2$) was determined to be equal to Securidine A minus four hydrogen atoms and two nitrogen atoms. Out of the isolated mono-brominated compounds, this would make MBC-339 the least likely to be a variant of Securidine A as removal of two nitrogen atoms would alter its core structure. This would have to be confirmed by NMR analysis and MBC-339 thus included further in the isolation campaign. Compound 373 was believed to have an additional oxygen atom based on its mass. However, compound 373 was discarded after the first purification process of extract M13065 due to low yield and purity. It was not successfully dereplicated and consequently terminated from further investigation. Other compounds with calculated elemental compositions which made them likely analogues, but only present in trace amount, were excluded from further analysis.

After identifying likely halogenated Securidine A analogues, other analogues that are often seen in samples containing multiple compounds with identical chemical scaffolds was pursued. The mass of a possible non-brominated analogue of MBC-340 with an added proton (bromine exchanged for hydrogen) was searched for and detected as MBC-342 (*m/z* 265). The elemental composition of MBC-342 was calculated to be $C_{13}H_{20}N_4O_2$ and it was suspected to be the debrominated version of MBC-340 (Figure 10).

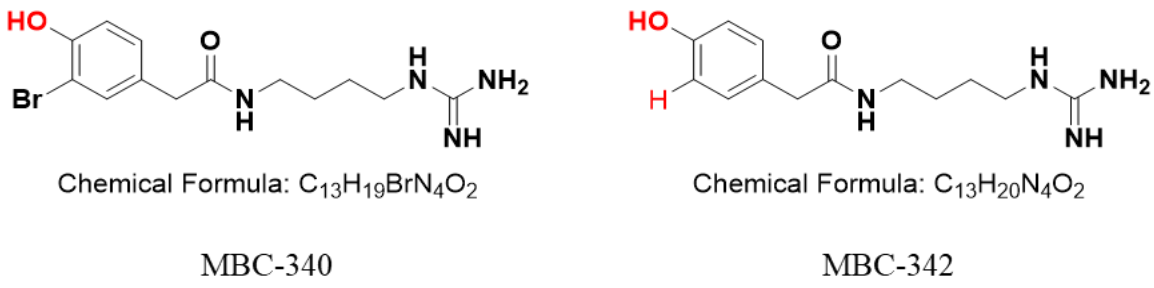

Figure 10 - Proposed structure of MBC-342 made by comparing the elemental composition of the compound to that of MBC-340.

4.4 Selection and dereplication of non-securidine related compounds

After the isolation method for Securidine A and its suspected analogues had been optimized, the obtained data from the preparative HPLC-MS system was analyzed to evaluate whether additional non-securidine related compounds could easily be isolated. This is a routine procedure at Marbio which requires minimal work when the isolation process is already being performed and could potentially reveal novel and bioactive compounds that otherwise would remain unnoticed. MBC-341 eluted as a distinct peak which looked viable for isolation and was therefore nominated as an additional target compound. A reliable calculated elemental composition was not obtained at the time but was determined following the second purification step of the compound. The elemental composition of MBC-341 was revealed to be $C_{17}H_{22}N_2O_7$. This elemental composition did not yield any hits during database searches and the compound was therefore suspected to be novel.

Out of the initial six target compounds, five of them were successfully dereplicated and provided accurate elemental compositions (Table 23).

Table 23 - Results from dereplication of target compounds. *Table includes compound name, observed mass $[M+H]^+$, neutral mass and calculated elemental composition.*

Compound name	Mass $[M+H]^+$	Neutral mass (Da)	Calculated elemental composition
Securidine A	357.0927	356.0848	$C_{14}H_{21}BrN_4O_2$
MBC-339	325.0554	324.0474	$C_{14}H_{17}BrN_2O_2$
MBC-340	343.0765	342.0691	$C_{13}H_{19}BrN_4O_2$
MBC-341	367.1502	366.1428	$C_{17}H_{22}N_2O_7$
MBC-342	265.1663	264.1589	$C_{13}H_{20}N_4O_2$

4.5 Isolation

Isolation of target compounds were completed using mass-guided semi-preparative HPLC. The isolation was achieved through a three-part process. The first part consisted of performing scouting runs on a selection of columns to aid in method optimization. Secondly, the initial purification step was designed to divide the target compounds into separate fractions. The final step was individually customized for each fraction to provide optimal purification and sufficient quantities of each target compound. Throughout the whole process, the same mobile phases were used. Mobile phase A consisted of ddH_2O with 0.1% FA, while mobile phase B consisted of ACN with 0.1% FA. For the remainder of section 4.5, the mobile phases will simply be referred to as A and B.

4.5.1 Method optimization

Isolation of natural products is time-consuming and labor-intensive. Unlike many other steps in the bioprospecting pipeline, it cannot be conducted in a high-throughput manner (Bucar et al., 2013) To ensure that the isolation protocol is performed as efficiently as possible, method optimization is essential.

Scouting runs was performed on extract M13065. The acquired information was used to select the best suited column and gradient for isolation of selected target compounds. This optimized method was tested and subsequently used on extract M19011 as well. When selecting a column for the initial purification step (four columns tested in Table 6 in section 3.5.1) the chromatograms were evaluated based on three main criteria:

- Peak of target masses (ideally Gauss-shaped)
- Separation of target compounds (no overlaps)
- Target compounds co-elutes with few impurities

The evaluation was based on analysis of the resulting base peak intensity (BPI) chromatogram from each column (Figure 11). BPI chromatograms were preferred to interpret individual performance and suitability, since it reduces the background noise from total ion current (TIC) chromatograms by only monitoring the most intense peak at any given moment. From the initial

evaluation, the Fluoro-phenyl column was excluded due to inadequate separation and uneven peaks compared to the other columns. The remaining columns were used to locate target compounds and evaluate them individually.

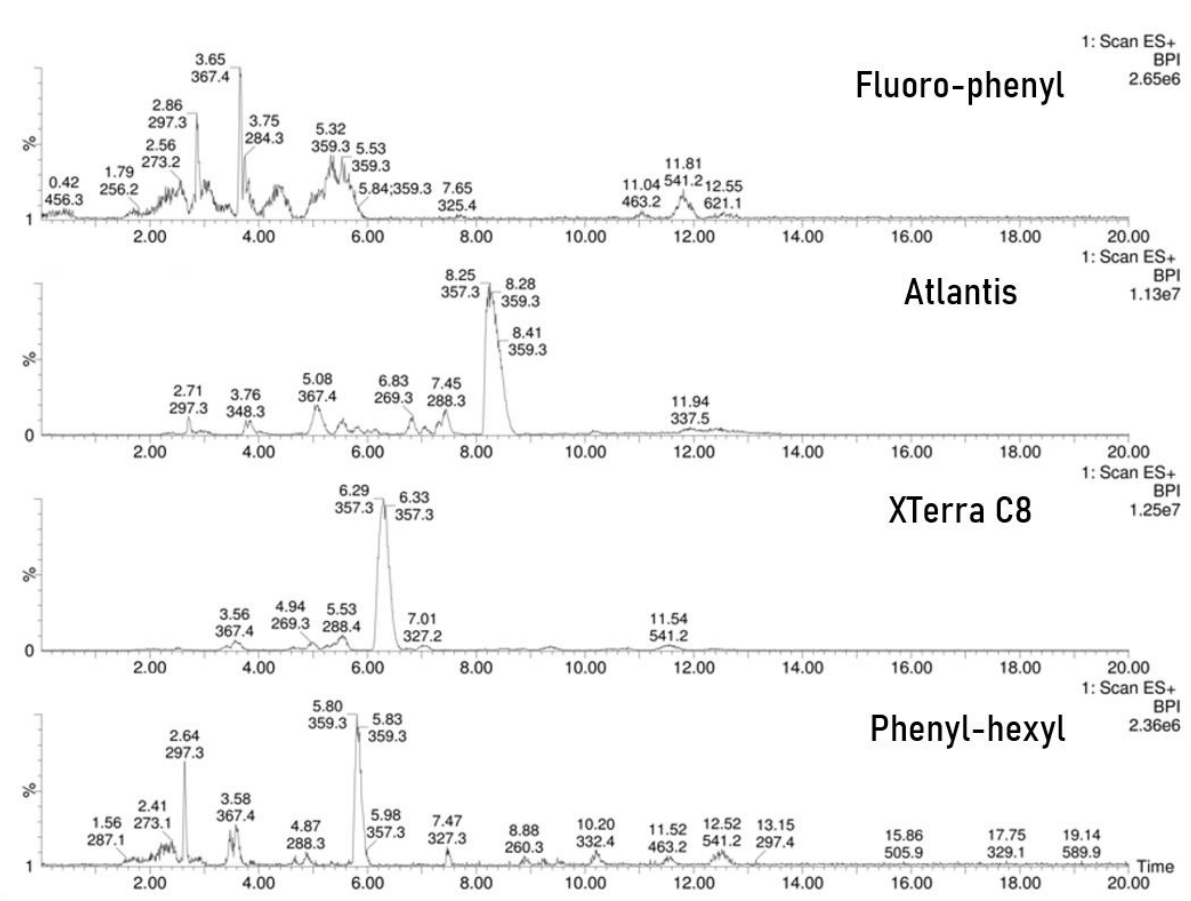

Figure 11 - BPI chromatograms from the scouting runs of four different columns. *The performance and suitability of each column were evaluated based on the three main criteria. Column Fluoro-phenyl was excluded from further analysis based on these criteria, due to dissatisfying peak-shape and separation.*

All three remaining columns presented reasonably well-shaped peaks and decent separation during the initial evaluation. When examining individual target compounds, the phenyl-hexyl column did not provide the same separation quality as the two other columns, and target compound 373 was not detected using this column. To assess the purity of each compound, integrated mass spectra for each peak was produced. The ideal results from this integration are peaks originating from the target compounds with no or few impurities present. An example of an integrated mass spectrum from Securidine A is shown in Figure 12.

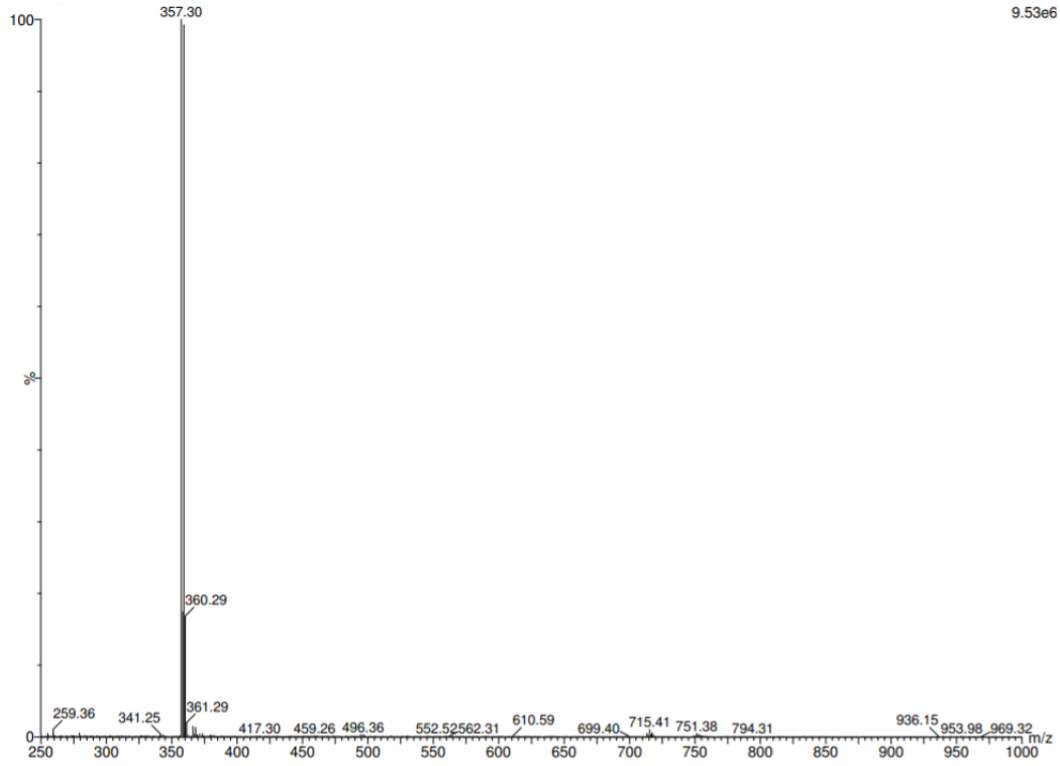

Figure 12 - Example of an integrated mass spectrum from Securidine A. *This example shows a very clean peak with close to no impurities.*

Ion chromatograms of co-eluting peaks were also produced to closely evaluate the separation between the individual peaks. For Atlantis®, target compounds Securidine A and MBC-339 were overlapping (Figure 13). XTerra® C8 provided the best separation of target compounds with no overlaps, as well as contributing to less pressure on the machinery due to its larger particle size and reduced wear and tear. XTerra® C8 was thus chosen as the most suitable column.

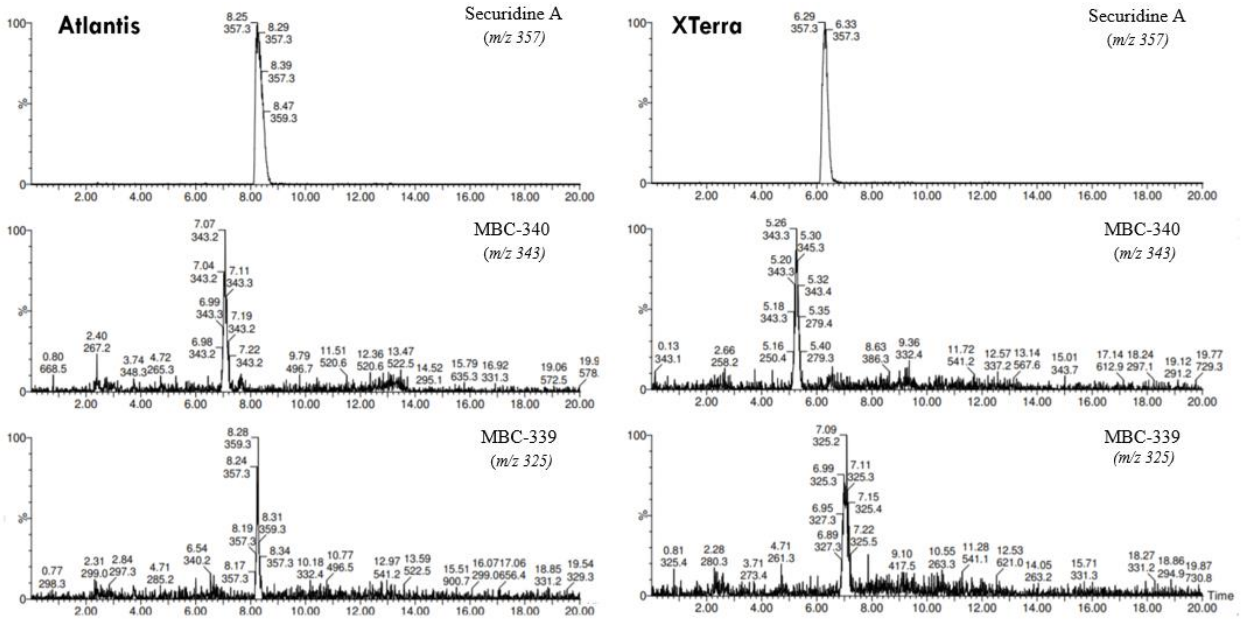

Figure 13 - Comparison between the Atlantis® and XTerra® C8 columns. *Each chromatogram shows when a specific target compound (Securidine A, MBC-340 and MBC-339) is eluted. An overlap between target compounds Securidine A and MBC-339 was discovered in the Atlantis column, making XTerra® C8 the column of choice.*

Based on the initial scouting run from the chosen column XTerra® C8, the gradient was shortened to 11 min with a linear progression of 0-58% of mobile phase B (Table 8, section 3.5.2). All components in the sample had already eluted at this point, and the separation of the target compounds were sufficient. Using a shorter gradient sped up the purification process and used less solvent, thus saving both time and expenses without affecting separation quality.

4.5.2 First purification step

The first purification step was performed using the optimized method. Each of the five target compounds were collected in separate fractions during this process (Figure 14). Fractions containing the same target compounds were pooled together and dried.

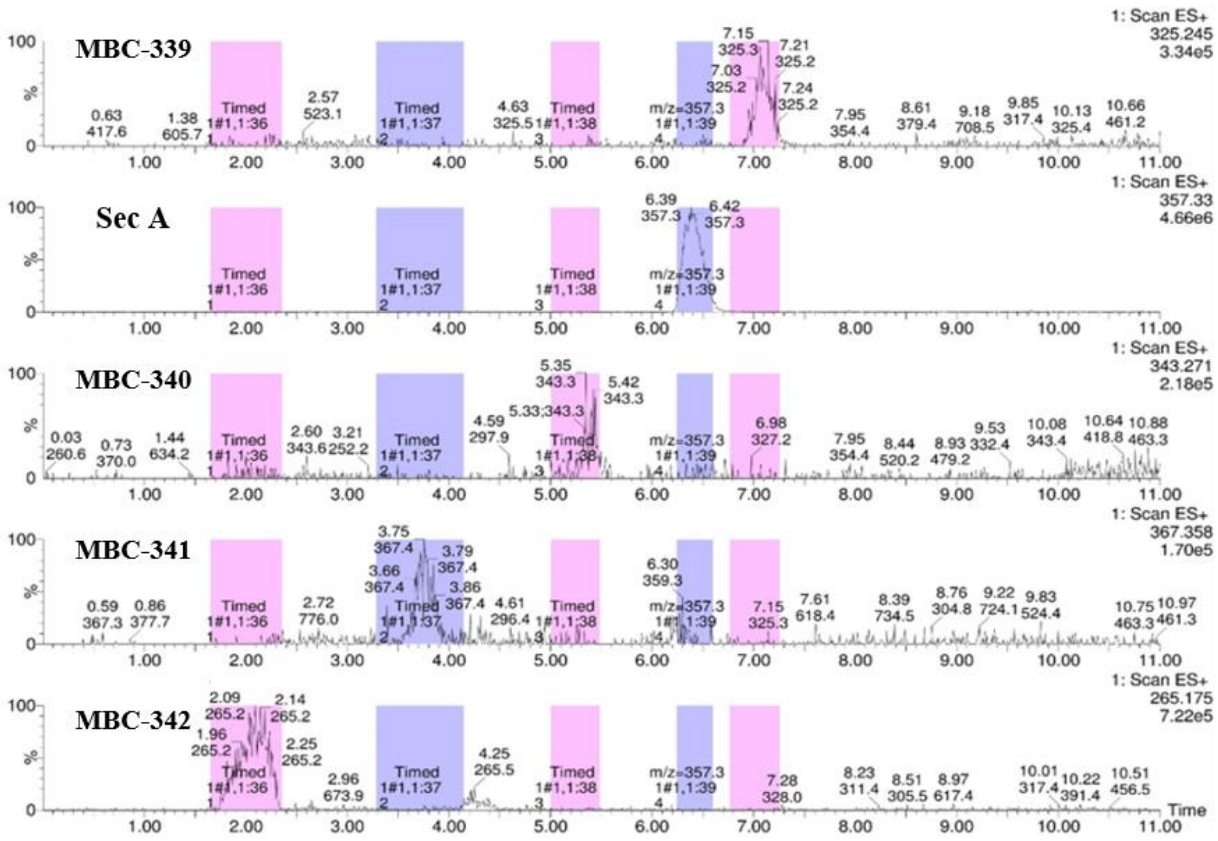

Figure 14 - Image of a standard purification run. *Each chromatogram shows the elution of a single target compound and each colored area represents a fraction. Each fraction contains the main peak of one of the target compounds. The example is from extract M13065.*

4.5.3 Second purification step

During the second purification step, the gradient was individually customized for each target compound to secure optimal isolation. The second purification was performed on a Waters® Acquity Arc system, using a smaller column and less solvent compared to the Waters® system used for the initial purification. This led to higher accuracy and provided purer samples at the expense of being more time-consuming and requiring more experimentation with gradient

composition, since no alternative columns were available at the time. Following the first purification, Securidine A was deemed pure enough for further analysis and additional purification was unnecessary (see Figure 12). The four remaining compounds underwent a second round of purification.

4.5.3.1 Second purification step of MBC-339

The gradient used for the second purification of MBC-339 was a linear gradient 0-40% B for 8 min, then washing and equilibration of the column for the final 5 min. The compound eluted at RT 7.78 with few contaminants (Figure 15).

One brominated fragment (*m/z* 265.89) was discovered in the mass spectrum of the collected sample (Figure 16). This could potentially be a degradation product or a fragment of the main compound. By some analyzing using UHPLC-ESI-HR-MS it was concluded to likely be a fragmentation caused by the ionization of the compound, since the presence of the fragment was even greater when exposed to higher energy ionization.

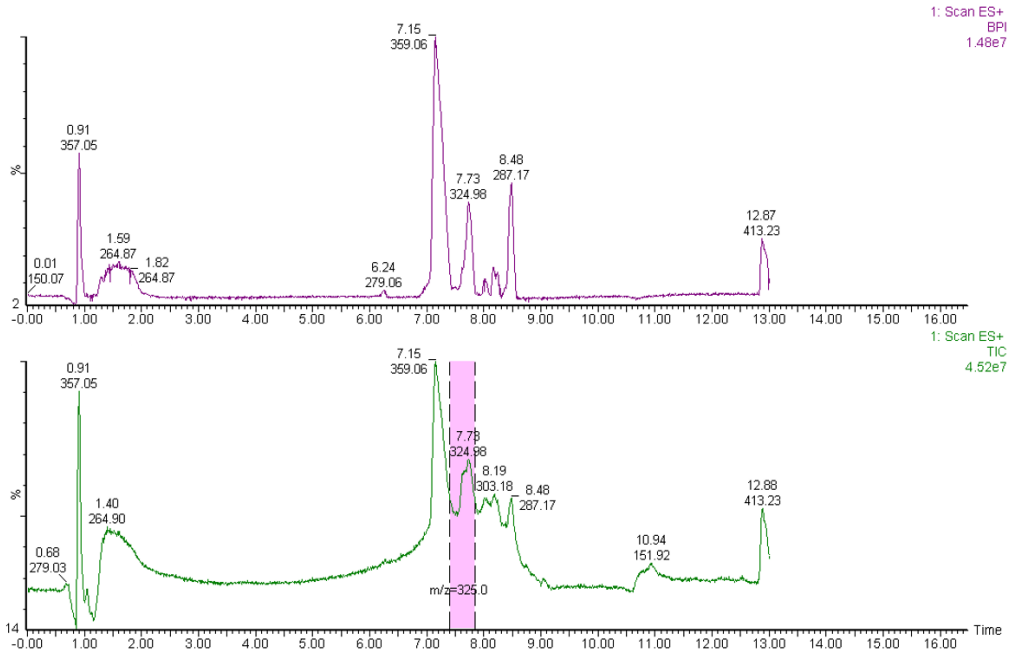

Figure 15 - Base peak intensity (BPI) and total ion current (TIC) chromatograms from the second purification of MBC-339 (m/z 325).

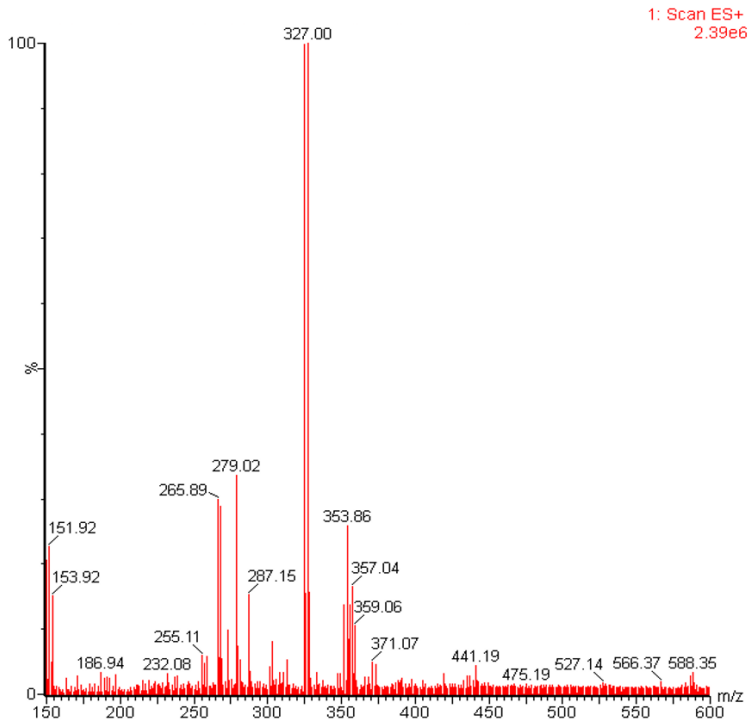

Figure 16 - Integrated mass spectrum of the peak from the second purification of MBC-339 (m/z 325).

4.5.3.2 Second purification step of MBC-340

The gradient used for second purification of MBC-340 was a linear gradient 0-25% B for 15 min, with washing steps for the final 6 min. The target compound eluted at RT 10.46 with few impurities (Figure 17).

The purification of MBC-340 was the most difficult one and required a lot of experimentation of gradient composition. The main issue was to separate the compound from the main contaminants with *m/z* 249 and 279 (Figure 18). This issue could likely have been solved faster with access to various columns, which unfortunately wasn't available at the time. Using the resulting gradient did eventually remove the main contaminant (*m/z* 249), while the presence of *m/z* 279 was significantly reduced.

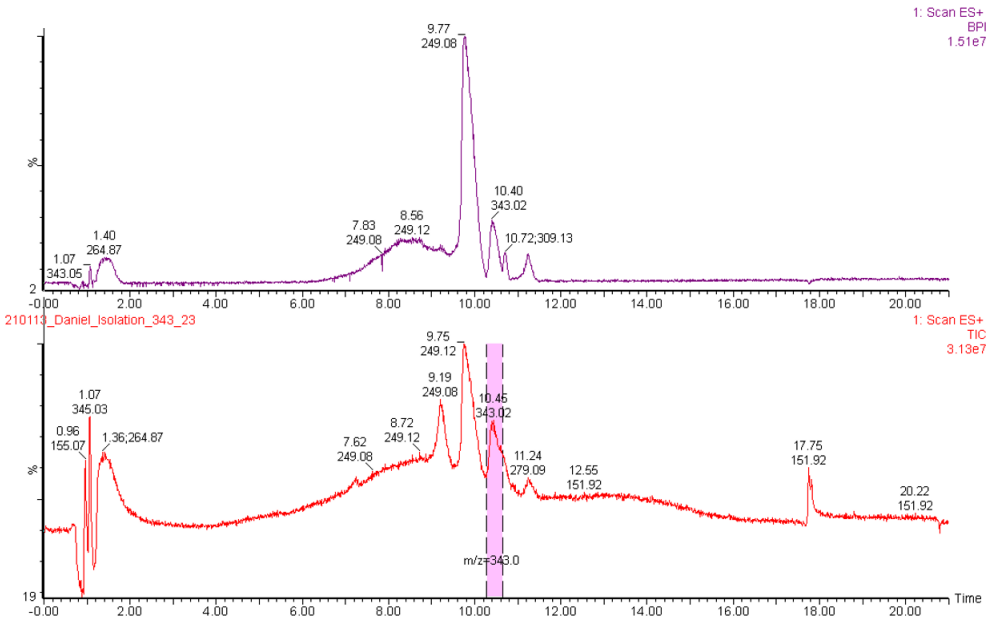

Figure 17 - BPI- and TIC-chromatograms from the second purification of MBC-340 (m/z 343).

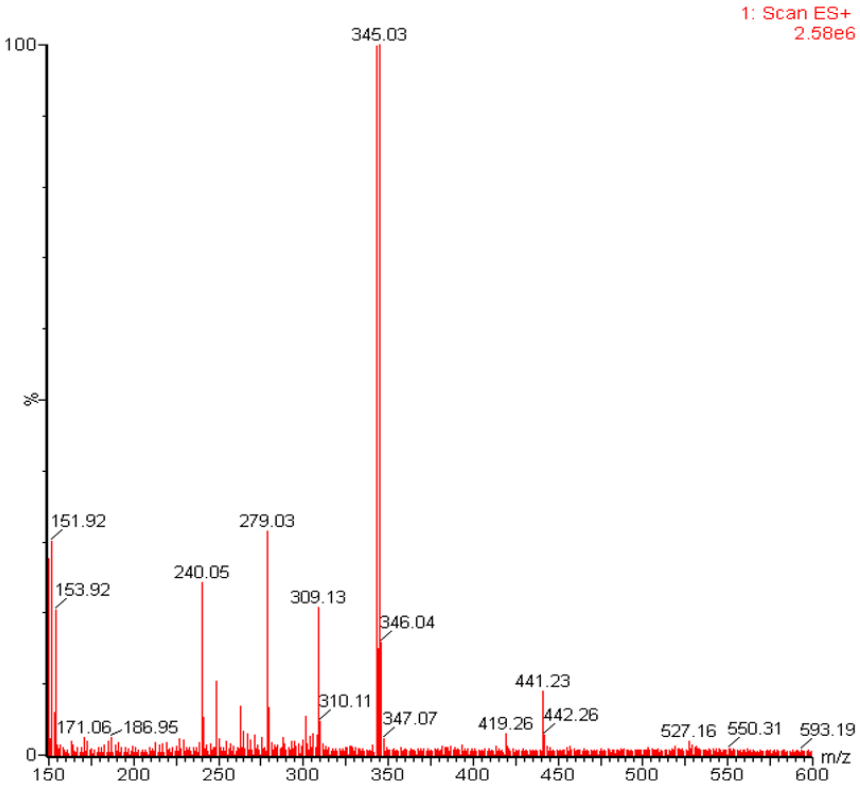

Figure 18 - Integrated mass spectrum of the peak from the second purification of MBC-340 (m/z 343).

4.5.3.3 Second purification step of MBC-341.

The gradient used for the second purification of MBC-341 consisted of an initial step with 100% A for 2 min, followed by a linear gradient 0-25% B for 8 min, then final washing and equilibration steps.

MBC-341 eluted at two different times (RT 6.55 and 9.27), which was unexpected since this was not previously experienced during the initial isolation (Figure 19). The peaks were collected separately and analyzed using UHPLC-ESI-HR-MS, which revealed that their elemental composition was identical, while the collision cross section (CCS) values for the two peaks were different. The peak at RT 6.55 registered a CCS-value of 187.38 $Å^2$, while the peak at RT 9.27 showed a CCS-value of 185.73 $Å^2$. The CCS value refers to how much drag the compound experience when it travels through a cell filled with nitrogen gas. The mass of a molecule is revealed by the *m/z*-ratio, while the CCS can provide additional information about the conformation of a compound (Hernández-Mesa et al., 2018). Since the CCS of the two variants of MBC-341 differed, while the *m/z* and the calculated elemental composition remained the same, it is possible that two structural isomers of the same compound were present in the sample.

Both fractions were analyzed in UHPLC-ESI-HR-MS to determine their purity. Fraction 1 (RT 6.55) had one main contaminant, while fraction 2 (RT 9.27) had several contaminants. Fraction 1 was significantly more purified than fraction 2 (Table 20). Therefore, only the first fraction was dried and used for further analyses and structure elucidation.

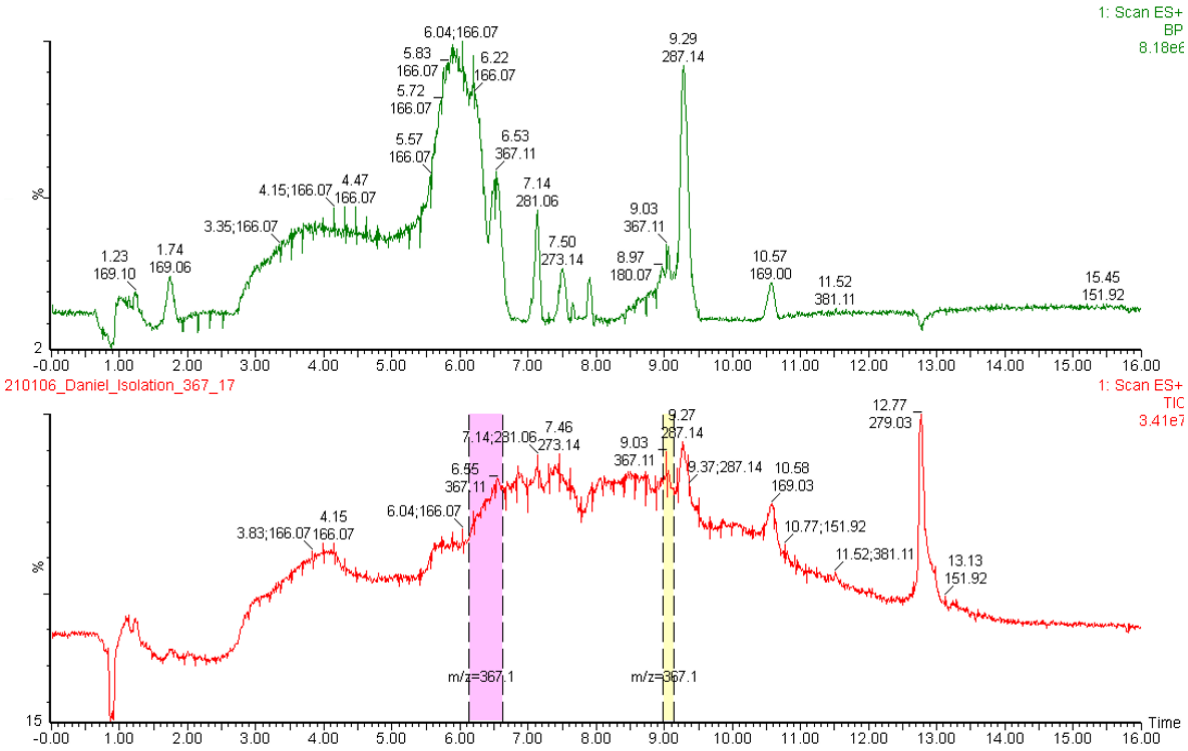

Figure 19 - BPI- and TIC-chromatograms from the second purification of MBC-341 (m/z 367).

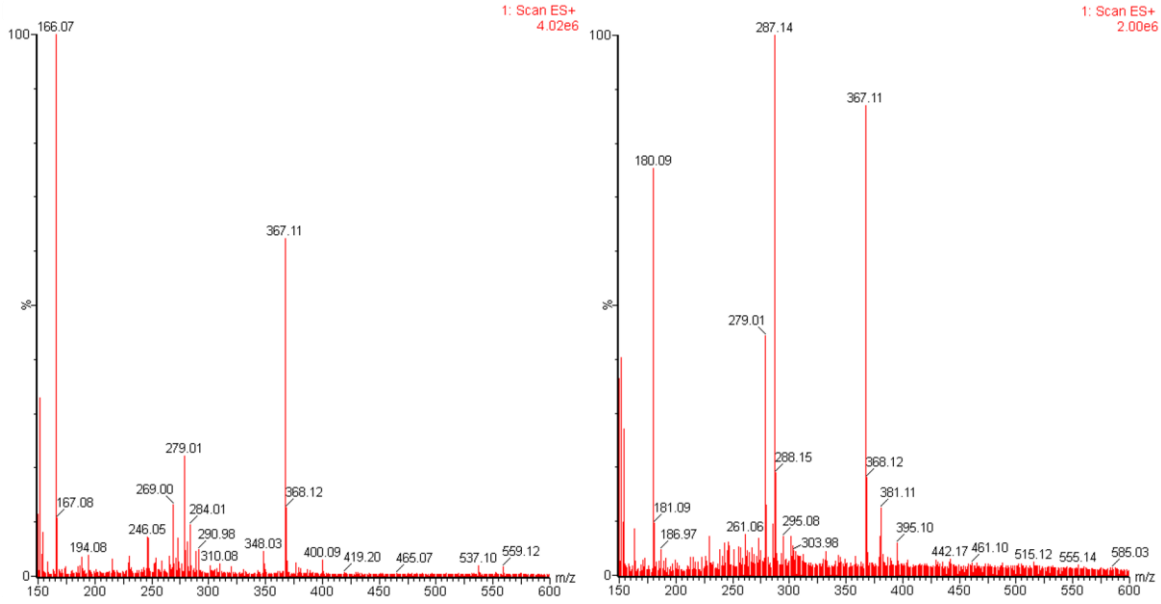

Figure 20 - Integrated mass spectrums of both fractions containing MBC-341 (m/z 367). *Fraction 1 (left) is mainly contaminated by compound 166.07, while fraction 2 (right) has several contaminants.*

4.5.3.4 Second purification step of MBC-342

The gradient used for second purification of MBC-342 was 100% A for 2 min, then a linear gradient 0-10% B for 8 min. The last 6 min were used to wash and equilibrate the column.

MBC-342 eluted at RT 9.32, but the compound also eluted at the beginning of the gradient, where only water was used as solvent (Figure 21). This part of the gradient was designed to remove salts, carbohydrates and other highly polar components from the extract, so the target compound was not expected to elute at this point. This could likely be due to flow-through of the column, which can occur when a percentage of the sample has not bound to the column material. The unbound compounds will proceed directly through the column without interruption and will therefore elute a lot earlier than expected. This could happen due to several reasons, one of the main reasons being an overload of the column. Attempts to lower the injection volume as well as performing a longer washing sequence did not fix the issue. Regardless, the peak that eluted at RT 9.32 looked to be relatively pure and undisturbed by the flow-through.

A comparison of the mass spectrums from both peaks is shown in Figure 22. UHPLC-ESI-HR-MS was performed on both fractions to confirm their purity. Only the fraction containing the main peak at RT 9.32 was dried and used for further analysis.

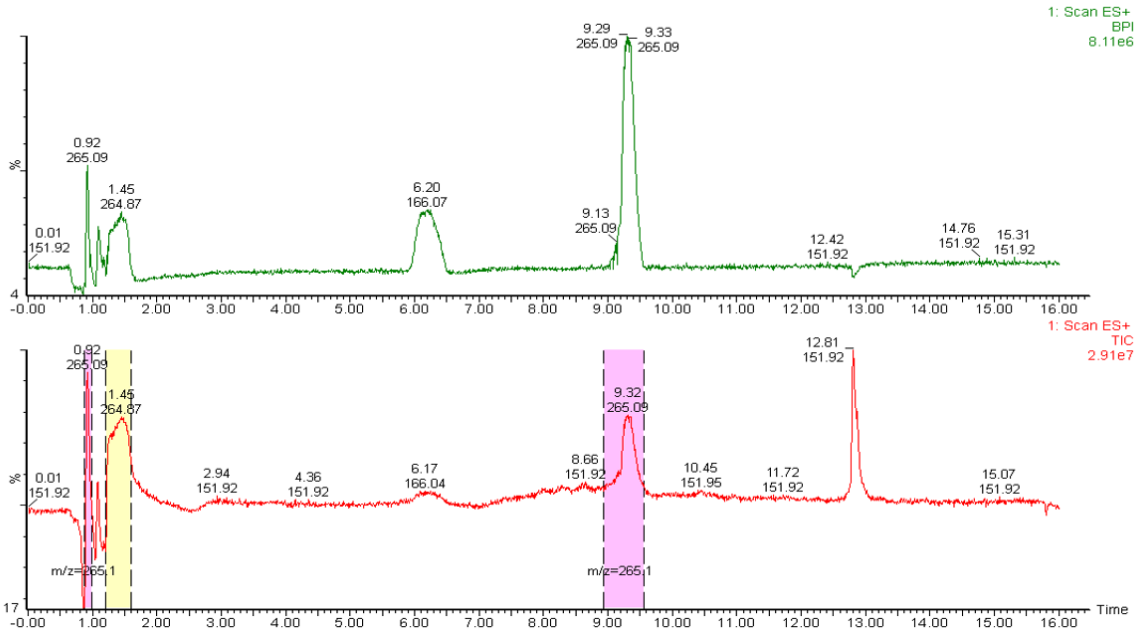

Figure 21 - BPI- and TIC-chromatograms from the second purification of MBC-342 (m/z 265).

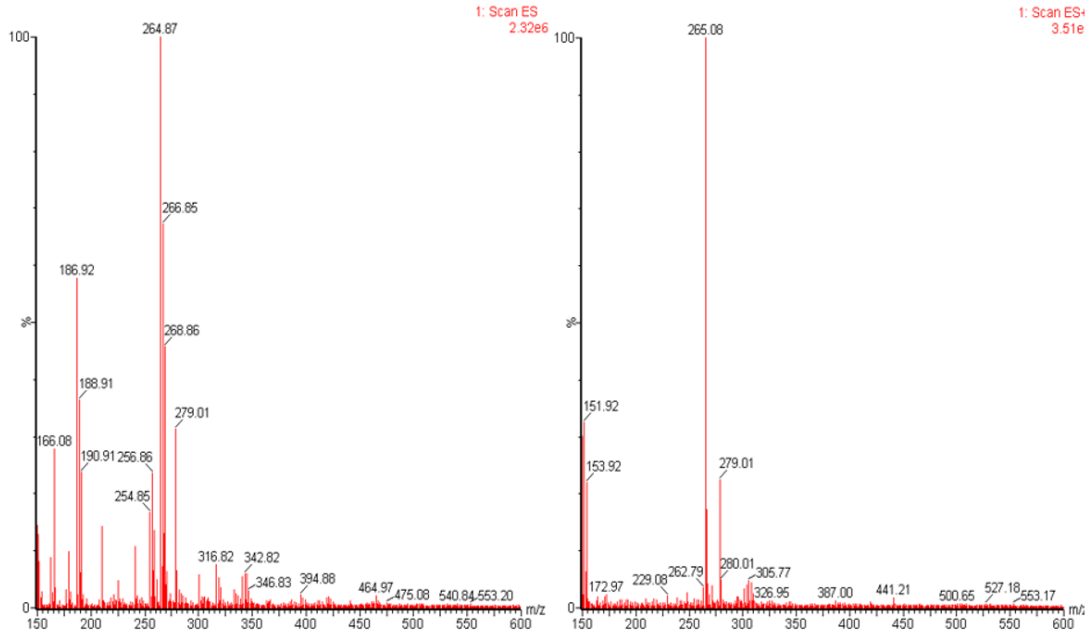

Figure 22 - Integrated mass spectrums of both fractions from MBC-342 (m/z 265). *The early peak at RT 1.45 (left) and the main peak at RT 9.32 (right).*

4.5.4 Yield of target compounds

A total of five target compounds, three believed to be analogues of Securidine A, were isolated using semi-preparative HPLC. Their weight was determined by pre-weighting a glass tube, freeze-drying the sample and remeasuring the weight (Table 24).

Table 24 - Yield of target compounds after isolation and freeze-drying. *Table also includes name, mass, pre- and post-weight of samples.*

Name	Mass	Pre-weight	Post-weight	Yield
Securidine A	357	5332.5 mg	5343.3 mg	10.8 mg
MBC-339	325	8748.2 mg	8749.6 mg	1.4 mg
MBC-340	343	5186.0 mg	5186.8 mg	0.8 mg
MBC-341	367	5319.0 mg	5320.3 mg	1.3 mg
MBC-342	265	5171.0 mg	5171.3 mg	0.3 mg

Securidine A clearly provided the highest yield with 10.8 mg. This was only collected from the first 2 g of dry weight from sample M13065, so there is potential to isolate relatively large amounts of the compound if required. For this project, a larger amount was not necessary.

The other isolated compounds varied from 0.3 mg to 1.4 mg in yield from approximately 7 g of dry weight. MBC-342 produced the lowest yield (0.3 mg). Because of the low amount, structure elucidation using NMR was deemed impossible and the compound was submitted directly to bioactivity testing. The remaining compounds were of sufficient yield for continuation for both structure elucidation with NMR and bioactivity testing.

4.6 Structure elucidation of target compounds

Three of the isolated compounds were sent to NMR for structure elucidation. These were the two mono-brominated compounds MBC-339 and MBC-340, as well as the non-brominated compound MBC-341. Structure elucidation using NMR was not possible for MBC-342 due to low yield (0.3 mg). MBC-342 was elucidated using fragmentation patterns provided by HR-MS instead. Securidine A was already identified during dereplication and not a priority for further confirmation due to time constraints.

4.6.1 Structure elucidation of MBC-339

The elemental composition of MBC-339 was calculated to be $C_{14}H_{17}BrN_2O_2$ based on HR-MS results. This entails that MBC-339 has four additional hydrogen atoms and two less nitrogen atoms compared to Securidine A ($C_{14}H_{21}BrN_4O_2$). This observed difference is challenging to explain simply by adding and removing these atom types from the Securidine A structure, as this would require changes to the core structure of Securidine A where all nitrogen atoms are found. This does not conclude that MBC-339 is structurally unrelated to Securidine A but can indicate that the compound has undergone chemical modification due to sample handling. Such degradation products are referred to as artifacts and are quite commonly seen in samples subjected to various solvents and changes in pH, temperatures and pressure (Capon, 2020).

NMR data for this compound was found inconclusive, but points in the direction of MBC-339 not having the same core structure as Securidine A. MBC-339 has a benzene ring consisting of four CH carbons, where the benzene ring of Securidine has three CH carbons (Figure 23). In addition, three substructures, CH-CH-CH_2, CH_2-CH_2 and CH_2-CH_2-CH_3, were also visible. These substructures cannot be found in Securidine A and point towards MBC-339 not being a Securidine A analogue nor an artefact thereof. The four substructures accounts for all the 14 carbon atoms of MBC-339, however the dataset failed to connect the substructures to each other. ROESY data indicates that the -CH-CH-CH_2- substructure is attached to the benzene ring through a quaternary carbon or a heteroatom (Appendix Figure A4). Additionally, no NH shifts were observed in the proton spectrum. Further NMR experiments are needed to determine the structure of the compound. HSQC and HMBC data of MBC-339 with elucidated substructures can be seen in Appendix Figure A3.

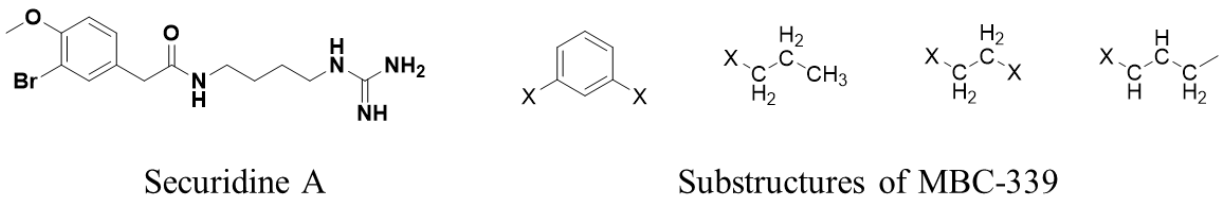

Figure 23 - Structure of Securidine A and the elucidated substructures of MBC-339.

4.6.2 Structure elucidation of MBC-340

The structure of MBC-340 was confirmed to be the demethylated variant of Securidine A by thorough analysis of NMR data (^{1}H, ^{13}C, HMBC, HSQC and COSY). NMR spectra of MBC-340 can be seen in Appendix Figures A5-A8. The elucidated structure with key 2D NMR correlations can be seen in Figure 24. The obtained chemical shift values can be seen in Table 25. For Securidine A, the 2-C methoxy group gave clear signals at C-1: 56.6 ppm and H_3-1: 3.84 (s). These signals were absent in the MBC-340 dataset. Due to the low amounts of MBC-340, only four out of the 14 carbon atoms were visible in the ^{13}C-spectrum. The shift values of nine of the remaining carbon atoms were extracted from HMBC data. The shift value of carbon atom C-2 could not be obtained. However, since all other carbons were assigned, the elucidated structure of MBC-340 remained the only option. The dataset revealed that the MBC-340 sample contains impurities. This resulted in overlapping for most peaks in the ^{1}H-spectrum. Multiplicity and coupling constants could therefore not be obtained for most of the protons. The bromine atom was placed on carbon atom C-5 due to its characteristic shift value. As a result, the structure of MBC-340 was elucidated as 2-(3-bromo-4-hydroxyphenyl)-*N*-(4-guanidinobutyl)acetamide.

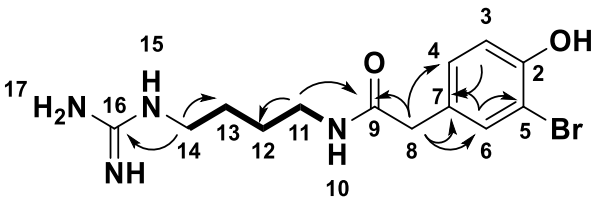

Figure 24 - Structure of MBC-340. *Black arrows = HMBC correlations, bold lines = COSY correlations*

Table 25 - ^{1}H and ^{13}C NMR assignments for MBC-340

Position	δc, type	δ_H (J in Hz)
2	n.d.	
3	115.9, C	6.90
4	128.6, C	7.24
5	153.2, C	
6	132.6, CH	7.34
7	128.9, C	
8	40.81, CH_2	3.26, s
9	170.3, C	
10	(NH)	8.09
11	38.2, CH_2	3.03[a]
12	25.83, CH_2[b]	1.42[c]
13	25.83, CH_2[b]	1.42[c]
14	39.8, CH_2	3.03[a]
15	(NH)	n.d.
16	147.8, C	
17	(NH_2)	n.d.

[a-c] Signals are overlapping

n.d. Not detected

4.6.3 Structure elucidation of MBC-341

The elemental composition of MBC-341 was calculated to be $C_{17}H_{22}N_2O_7$ based on HR-MS analysis. This compound was not suspected of being a Securidine A analogue, but rather an unrelated, novel compound. The isolated amount of MBC-341 was 1.3 mg. This low amount is pushing the limits in terms of recording NMR data that will allow full structure elucidation. To further complicate the structure elucidation, NMR data showed that the sample was not pure (HSQC and HMBC spectra combined in Figure 25). In Figure 25 all the blue peaks represent a CH_2 group and all the red peaks represents a CH or a CH_3 group. As the elemental composition of MBC-341 was calculated to be $C_{17}H_{22}N_2O_7$, it is clear that this sample contains several impurities contributing to all these signals. To elucidate the structure of MBC-341, additional purification steps would have to be run to enable NMR analysis of a sufficiently pure sample.

While this would bring the amount of sample available to analyze by NMR further down, this can be compensated by running more scans.

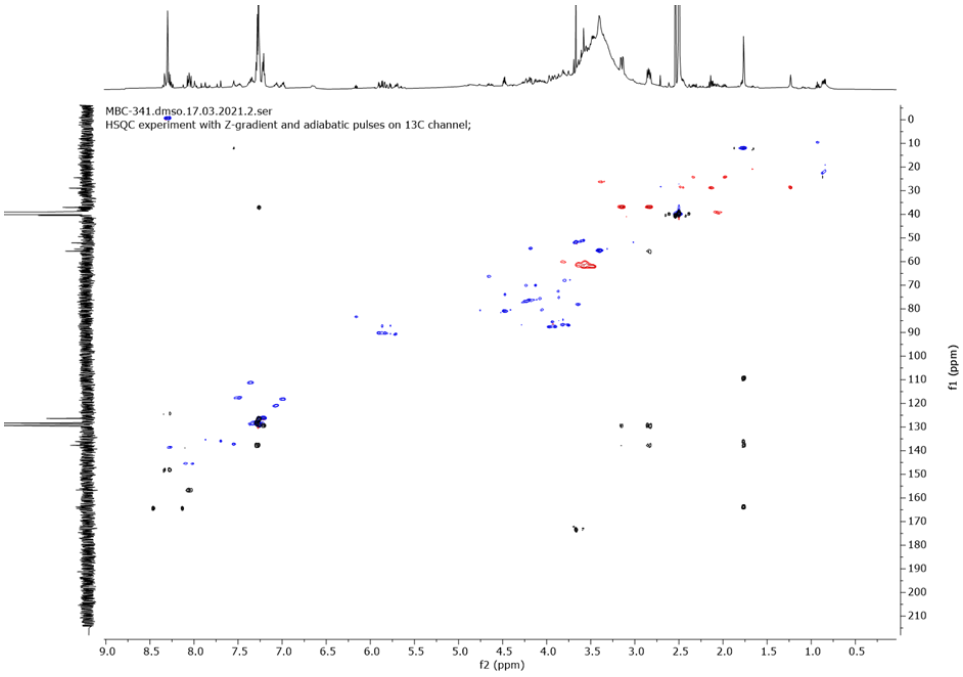

Figure 25 - HSQC and HMBC data recorded for MBC-341 (blue peaks = CH_2 groups, red peaks = CH or CH_3 groups).

4.6.4 Structure elucidation of MBC-342

The structure of MBC-342 was elucidated by analyzing the calculated elemental compositions of fragments provided by UHPLC-ESI-HR-MS and by comparisons to the structure of MBC-340 solved by NMR. This was done since the yield of MBC-342 was not sufficient for structure elucidation via NMR. The spectral information obtained from two experiments is shown in Appendix Figures A1-A2. From the acquired signals, the elemental compositions of three fragments were calculated and used to elucidate the structure of MBC-342 (Table 26).

Table 26 - Fragments used to elucidate the structure of MBC-342.

Fragment	*m/z*	Calculated elemental composition
1	248.13975	$C_{13}H_{17}N_3O_2$
2	206.11789	$C_{12}H_{15}NO_2$
3	107.04833	C_7H_6O

The elemental composition of MBC-342 has been calculated to be $C_{13}H_{20}N_4O_2$. Fragment 1 indicates a neutral loss of -H/-NH_2, while fragment 2 reveals neutral a loss of -H/-Guanidine (CH_4N_3). Fragment 3 obtained at a higher collision energy indicates that the second oxygen is located on the benzene ring, since no other assignment can explain the elemental composition of the fragment within the structural restrictions of a securidine. MBC-342 was thus confirmed to be the debrominated version of MBC-340 (Figure 26).

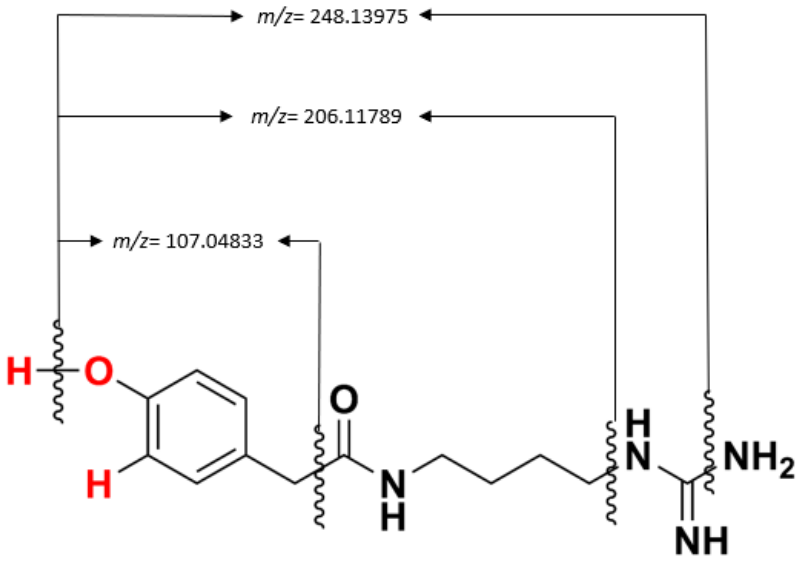

Figure 26 - Structure of MBC-342. *The three fragments used to elucidate the structure is marked.*

4.7 Bioactivity of target compounds

Bioactivity testing were performed on the five isolated compounds. The compounds were tested at 50 µM in three technical replicates for cytotoxic, antibacterial, antifungal, antidiabetic and antibiofilm formation effects (methods in section 3.8).

During the initial screening, compound MBC-340 showed activity against the malignant human melanoma cell line A2058. The quantitative assay IC_{50} was performed with a dilution series of various concentrations between 150 µM to 1.25 µM in order to determine the half-maximal inhibitory concentration of MBC-340 against the cancer cell line. Based on the obtained results, the IC_{50}-value of MBC-340 against cell line A2058 was determined to be around 110 µM (Figure 27). Since the measured concentration of MBC-340 did not result in cell survival rates below 40%, a full statistical analysis to determine the precise IC_{50}-value could not be performed using a software like GraphPad Prism. Therefore, the IC_{50}-value is stipulated from the graph in Figure 27. The compound was not assayed at higher concentrations due to the restricted amounts of MBC-340. While the measured data confirms that MBC-340 is indeed active against A2058, the activity is rather weak. An IC_{50} value of 110 µM is far above the concentrations that commercially available pharmaceuticals are active at, where the IC_{50}-values against their target cell lines typically resides in the nM range (Varbanov et al., 2017). Getting the activity of MBC-340 down to these levels would require significant medicinal chemistry efforts.

No steep drops in % survival was seen from one concentration point to the next. This indicates that MBC-340 is hitting a specific cellular target, rather than exerting general cytotoxicity (e.g. by targeting the cell membrane). This hypothesis is strengthened by the fact that the viability of MRC-5 (non-malignant lung tissue) was not affected by MBC-340. Determination of the mode-of-action of MBC-340 was beyond the scope of this thesis.

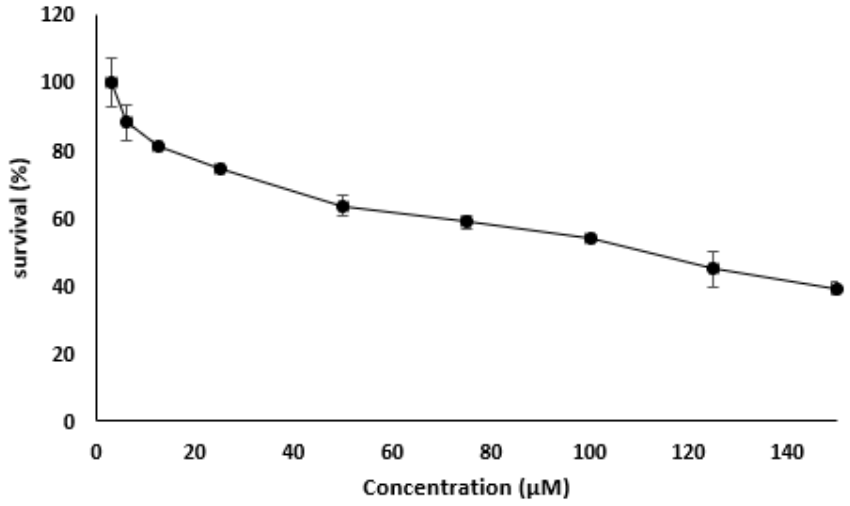

Figure 27 - Cytotoxicity of MBC-340 against the malignant cell line A2058.

The activity detected from MBC-340, which is the demethylated variant of Securidine A, shows that minor chemical differences can affect the bioactive properties of a compound.

None of the isolated compounds did show any significant antibacterial, antifungal, antidiabetic or antibiofilm formation effects at the tested concentration. MBC-340 was not effective against the non-malignant cell line MRC-5 at 50 µM. It is however possible that activity would be observed with increased compound concentration.

5 Conclusion

Four compounds suspected to be structurally related to Securidine A was identified in two extracts of the marine bryozoan *Securiflustra securifrons*. Three of these compounds (MBC-339, MBC-340, MBC-342) were successfully isolated, alongside Securidine A and one non-securidine related compound (MBC-341). An optimized method for isolation of Securidine A was established during this work. All compounds were isolated in amounts sufficient for further biological characterization. MBC-339, MBC-340 and MBC-341 were isolated in sufficient amounts to allow for structure elucidation via NMR analysis. The structure of MBC-342 had to be confirmed via analysis of fragmentation patterns by HR-MS due to low yield (0.3 mg).

Structures of the novel securidine analogues MBC-340 and MBC-342 were revealed during this work. MBC-340 was confirmed to be the demethylated variant of Securidine A, while MBC-342 was the debrominated variant of MBC-340. Structure elucidation of MBC-339 and MBC-342 remained inconclusive. Substructures of MBC-339 were successfully obtained and indicated that the compound was not an analogue of Securidine A as originally thought. Additional efforts are needed to acquire the complete structures of MBC-339 and MBC-341. The securidine analogue MBC-340 did show activity against the malignant cancer cell line A2058. The IC_{50}-value was determined to be around 110 µM. No compounds showed any significant antibacterial, antifungal, antidiabetic or antibiofilm formation effects at a concentration of 50 µM.

The results in this thesis shows:

- That secondary metabolites from marine bryozoans can be a rich source of new, possibly bioactive, chemical structures.
- The importance of dereplication and optimized isolation methods to streamline the bioprospecting work.
- That isolation of analogues can uncover bioactive properties in molecules with only minor chemical differences.
- That natural products should be tested broadly to uncover their bioactivity.

6 References

Altmann, K. H. (2017). Drugs from the Oceans: Marine Natural Products as Leads for Drug Discovery. *Chimia (Aarau), 71*(10), 646-652. doi:10.2533/chimia.2017.646

Amon, A. (2015). A Case for More Curiosity-driven Basic Research. *Molecular Biology of the Cell, 26*(21), 3690-3691. doi:10.1091/mbc.e15-06-0430

Anthoni, U., Bock, K., Chevolot, L., Larsen, C., Nielsen, P. H., & Christophersen, C. (1987). Chartellamide A and B, Halogenated Beta-lactam Indole-imidazole Alkaloids from the Marine Bryozoan Chartella papyracea. *The Journal of Organic Chemistry, 52*(25), 5638-5639. doi:10.1021/jo00234a028

Appleton, D. R., Buss, A. D., & Butler, M. S. (2007). A Simple Method for High-Throughput Extract Prefractionation for Biological Screening. *CHIMIA International Journal for Chemistry, 61*(6), 327-331. doi:10.2533/chimia.2007.327

Appendino, G., Fontana, G., & Pollastro, F. (2010). Natural Products Drug Discovery. In Mander, L. & Liu, H. (Eds.) *Comprehensive Natural Products II Chemistry and Biology* (pp. 205-236): Elsevier

Appiah, B., Amponsah, I. K., Poudyal, A., & Mensah, M. L. K. (2018). Identifying Strengths and Weaknesses of the Integration of Biomedical and Herbal Medicine Units in Ghana Using the WHO Health Systems Framework: A qualitative study. *BMC Complementary and Alternative Medicine, 18*(1), 286-286. doi:10.1186/s12906-018-2334-2

Atanasov, A. G., Waltenberger, B., Pferschy-Wenzig, E.-M., Linder, T., Wawrosch, C., Uhrin, P., . . . Stuppner, H. (2015). Discovery and Resupply of Pharmacologically Active Plant-derived Natural Products: A Review. *Biotechnology Advances, 33*(8), 1582-1614. doi:10.1016/j.biotechadv.2015.08.001

Batta, A., Kalra, B. S., & Khirasaria, R. (2020). Trends in FDA Drug Approvals Over Last 2 Decades: An observational study. *Journal of Family Medicine and Primary Care*, *9*(1), 105–114. https://doi.org/10.4103/jfmpc.jfmpc_578_19

Beattie, A. J., Hay, M., Magnusson, B., De Nys, R., Smeathers, J., & Vincent, J. F. V. (2011). Ecology and Bioprospecting. *Austral Ecology, 36*(3), 341-356. doi:10.1111/j.1442 9993.2010.02170.x

Berk, Z. (2018). Chapter 11 - Extraction. In Z. Berk (Ed.), *Food Process Engineering and Technology (Third Edition)* (pp. 289-310): Academic Press.

Bernardini, S., Tiezzi, A., Laghezza Masci, V., & Ovidi, E. (2018). Natural Products for Human Health: An Historical Overview of the Drug Discovery Approaches. *Natural Product Research, 32*(16), 1926-1950. doi:10.1080/14786419.2017.1356838

Biggs, R. (2005). Medicine, Surgery, and Public Health in Ancient Mesopotamia. *Journal of Assyrian Academic Studies, 19*(1), 7-18.

Blunt, J. W., Carroll, A. R., Copp, B. R., Davis, R. A., Keyzers, R. A., & Prinsep, M. R. (2018). Marine natural products. *Natural Product Reports, 35*(1), 8-53. doi:10.1039/c7np00052a

Bock, P., Gordon, D. & Hayward, P. (2020). World List of Bryozoa. *Securiflustra securifrons* (Pallas, 1776). Accessed November 2020 at World Register of Marine Species http://www.marinespecies.org/aphia.php?p=taxdetails&id=111374

Breitling, R., & Takano, E. (2016). Synthetic Biology of Natural Products. *Cold Spring Harbor Perspectives in Biology, 8*(10), a023994. doi:10.1101/cshperspect.a023994

Bucar, F., Wube, A., & Schmid, M. (2013). Natural Product Isolation – How to get From Biological Material to Pure Compounds. *Natural Product Reports, 30*(4), 525-545. doi:10.1039/C3NP20106F

Campbell, N.A., Reece, J.B., Urry, L.A., Cain, M.L., Wassermann, S.A., Minorsky, P.V. & Jackson, R.N (2015). Chapter 33 - Invertebrates. In, *Biology - A Global Approach (Tenth edition)* (pp. 743 - 773). Pearson Global Edition

Capon, R. J. (2020). Extracting Value: Mechanistic Insights into the Formation of Natural Product Artifacts – Case Studies in Marine Natural Products. *Natural Product Reports, 37*(1), 55-79. doi:10.1039/C9NP00013E

Chevolot, L., Chevolot, A. M., Gajhede, M., Larsen, C., Anthoni, U., & Christophersen, C. (1985). Chartelline A: A Pentahalogenated Alkaloid From the Marine Bryozoan *Chartella papyracea*. *Journal of the American Chemical Society, 107*(15), 4542-4543. doi:10.1021/ja00301a027

Choudhary, A., Naughton, L. M., Montánchez, I., Dobson, A. D. W., & Rai, D. K. (2017). Current Status and Future Prospects of Marine Natural Products (MNPs) as Antimicrobials. *Marine Drugs, 15*(9). doi:10.3390/md15090272

Debashish, G., Malay, S., Barindra, S., & Joydeep, M. (2005). Marine Enzymes. *Advances in Biochemical Engineering/Biotechnology, 96*, 189-218. doi:10.1007/b135785

Demain, A., & Fang, A. (2000). The Natural Functions of Secondary Metabolites. *Advances in Biochemical Engineering/Biotechnology*, *69*, 1-39.

Dong, M. W., & Zhang, K. (2014). Ultra-high-pressure Liquid Chromatography (UHPLC) in Method Development. *TrAC Trends in Analytical Chemistry*, *63*, 21-30. doi:https://doi.org/10.1016/j.trac.2014.06.019

Duarte, A. W. F., Dos Santos, J. A., Vianna, M. V., Vieira, J. M. F., Mallagutti, V. H., Inforsato, F. J., . . . Durães Sette, L. (2018). Cold-adapted Enzymes Produced by Fungi from Terrestrial and Marine Antarctic Environments. *Critical Reviews in Biotechnology, 38*(4), 600-619. doi:10.1080/07388551.2017.1379468

Feher, M., & Schmidt, J. M. (2003). Property Distributions: Differences between Drugs, Natural Products, and Molecules from Combinatorial Chemistry. *Journal of Chemical Information and Computer Sciences, 43*(1), 218-227. doi:10.1021/ci0200467

Grischenko, A. V., & Chernyshev, A. V. (2018). Deep-water Bryozoa from the Kuril Basin, Sea of Okhotsk. *Deep Sea Research Part II: Topical Studies in Oceanography, 154*, 59-73. doi:10.1016/j.dsr2.2017.09.011

Haefner, B. (2003). Drugs from the Deep: Marine Natural Products as Drug Candidates. *Drug Discovery Today, 8*(12), 536-544. doi:10.1016/s1359-6446(03)02713-2

Hansen, K. Ø., Andersen, J. H., Bayer, A., Pandey, S. K., Lorentzen, M., Jørgensen, K. B., . . . Hansen, E. H. (2019). Kinase Chemodiversity from the Arctic: The Breitfussins. *Journal of Medicinal Chemistry, 62*(22), 10167-10181. doi:10.1021/acs.jmedchem.9b01006

Hansen, K. Ø., Isaksson, J., Bayer, A., Johansen, J. A., Andersen, J. H., & Hansen, E. (2017). Securamine Derivatives from the Arctic Bryozoan *Securiflustra securifrons*. *Journal of Natural Products, 80*(12), 3276-3283. doi:10.1021/acs.jnatprod.7b00703

Harvey, A. L., Edrada-Ebel, R., & Quinn, R. J. (2015). The Re-emergence of Natural products for Drug Discovery in the Genomics Era. *Nature Reviews Drug Discovery, 14*(2), 111-129. doi:10.1038/nrd4510

Hernández-Mesa, M., Le Bizec, B., Monteau, F., García-Campaña, A. M., & Dervilly-Pinel, G. (2018). Collision Cross Section (CCS) Database: An Additional Measure to Characterize Steroids. *Analytical Chemistry, 90*(7), 4616-4625. doi:10.1021/acs.analchem.7b05117

Ho, C. S., Lam, C. W., Chan, M. H., Cheung, R. C., Law, L. K., Lit, L. C., Ng, K. F., Suen, M. W., & Tai, H. L. (2003). Electrospray Ionisation Mass Spectrometry: Principles and Clinical Applications. *The Clinical Biochemist Reviews, 24*(1), 3–12.

Huang, K.-C., Su, Y.-C., Sun, M.-F., & Huang, S.-T. (2018). Chinese Herbal Medicine Improves the Long-Term Survival Rate of Patients With Chronic Kidney Disease in Taiwan: A Nationwide Retrospective Population-Based Cohort Study. *Frontiers in Pharmacology, 9*, 1117-1117. doi:10.3389/fphar.2018.01117

Hubert, J., Nuzillard, J.-M., & Renault, J.-H. (2017). Dereplication Strategies in Natural Product Research: How Many Tools and Methodologies Behind the Same Concept? *Phytochemistry Reviews, 16*(1), 55-95. doi:10.1007/s11101-015-9448-7

Hunt, B., & Vincent, A. C. J. (2006). Scale and Sustainability of Marine Bioprospecting for Pharmaceuticals. *AMBIO: A Journal of the Human Environment, 35*(2), 57-64. doi:10.1579/0044-7447(2006)35[57:sasomb]2.0.co;2

Kildgaard, S., Subko, K., Phillips, E., Goidts, V., de la Cruz, M., Díaz, C., . . . Larsen, T. O. (2017). A Dereplication and Bioguided Discovery Approach to Reveal New Compounds from a Marine-Derived Fungus *Stilbella fimetaria*. *Marine drugs, 15*(8), 253. doi:10.3390/md15080253

Kleks, G., Duffy, S., Lucantoni, L., Avery, V. M., & Carroll, A. R. (2020). Orthoscuticellines A–E, β-Carboline Alkaloids from the Bryozoan *Orthoscuticella ventricosa* Collected in Australia. *Journal of Natural Products, 83*(2), 422-428. doi:10.1021/acs.jnatprod.9b00933

Koehn, F. E., & Carter, G. T. (2005). The Evolving Role of Natural Products in Drug Discovery. *Nature Reviews Drug Discovery, 4*(3), 206-220. doi:10.1038/nrd1657

Koletić, N., Novosel, M., Rajević, N., & Franjević, D. (2015). Bryozoans are Returning Home: Recolonization of Freshwater Ecosystems Inferred from Phylogenetic Relationships. *Ecology and Evolution, 5*(2), 255-264. doi:10.1002/ece3.1352

Kuklinski, P. (2009). Ecology of Stone-encrusting Organisms in the Greenland Sea: A Review. *Polar Research, 28*(2), 222-237. doi:10.1111/j.1751-8369.2009.00105.x

Kurosaki, F. (2012). Induction and Activation of Plant Secondary Metabolism by External Stimuli. In Vallisuta, O. (Ed.), *Drug Discovery Research in Pharmacognosy* (pp. 209-226). InTech doi: 10.5772/31860

Lambert, J. B., Mazzola, E. P. & Ridge, C. D. (2019). *Nuclear Magnetic Resonance Spectroscopy: An Introduction to Principles, Applications, and Experimental Methods, 2nd Edition.* Wiley.

Latif, Z., & Sarker, S. D. (2012). Isolation of Natural Products by Preparative High Performance Liquid Chromatography (Prep-HPLC). In Sarker S., Nahar L. (eds) *Natural Products Isolation. Methods in Molecular Biology (Methods and Protocols), vol 864* (pp. 255 274): Humana Press. https://doi.org/10.1007/978-1-61779-624-1_10

Lindequist, U. (2016). Marine-Derived Pharmaceuticals - Challenges and Opportunities, *Biomolecules & Therapeutics*, 24(6), 561-571. doi: 10.4062/biomolther.2016.181

Loureiro, D. R. P., Soares, J. X., Costa, J. C., Magalhães, Á. F., Azevedo, C. M. G., Pinto, M. M. M., & Afonso, C. M. M. (2019). Structures, Activities and Drug-Likeness of Anti Infective Xanthone Derivatives Isolated from the Marine Environment: A Review. *Molecules (Basel, Switzerland), 24*(2), 243. doi:10.3390/molecules24020243

Lysek, N., Rachor, E., & Lindel, T. (2002). Isolation and Structure Elucidation of Deformylflustrabromine from the North Sea Bryozoan Flustra foliacea. *Zeitschrift für Naturforschung C, 57*(11-12), 1056-1061. doi:10.1515/znc-2002-11-1218

Maghembe, R., Damian, D., Makaranga, A., Nyandoro, S. S., Lyantagaye, S. L., Kusari, S., & Hatti-Kaul, R. (2020). Omics for Bioprospecting and Drug Discovery from Bacteria and Microalgae. *Antibiotics (Basel, Switzerland), 9*(5), 229. doi:10.3390/antibiotics9050229

Mateo, N., Nader, W., & Tamayo, G. (2001). Bioprospecting. In *Encyclopedia of Biodiversity* (pp. 471-488).

Mayer, A.M., Glaser, K. B., Cuevas, C., Jacobs, R. S., Kem, W., Little, R. D., McIntosh, J.M, Newman, D.J., Potts, B.C. & Shuster, D. E. (2010). The Odyssey of Marine Pharmaceuticals: A Current Pipeline Perspective. *Trends in Pharmacological Sciences, 31*(6), 255-265. doi:10.1016/j.tips.2010.02.005 (original publisher review) Accessed from https://www.marinepharmacology.org/aproved, accessed April 2021.

Michael, P., Hansen, K., Isaksson, J., Andersen, J., & Hansen, E. (2017). A Novel Brominated Alkaloid Securidine A, Isolated from the Marine Bryozoan *Securiflustra securifrons*. *Molecules, 22*(7), 1236. doi:10.3390/molecules22071236

Miljanich, G. P. (2004). Ziconotide: Neuronal Calcium Channel Blocker for Treating Severe Chronic Pain. *Current Medical Chemistry, 11*(23), 3029-3040. doi:10.2174/0929867043363884

Morales Duque, H., Campos Dias, S., & Franco, O. L. (2019). Structural and Functional Analyses of Cone Snail Toxins. *Marine drugs, 17*(6), 370. doi:10.3390/md17060370

Muigg, P., Rosén, J., Bohlin, L., & Backlund, A. (2013). In silico Comparison of Marine, Terrestrial and Synthetic Compounds Using ChemGPS-NP for Navigating Chemical Space. *Phytochemistry Reviews, 12*(3), 449-457. doi:10.1007/s11101-012-9256-2

Newman, D. J., & Cragg, G. M. (2020). Natural Products as Sources of New Drugs over the Nearly Four Decades from 01/1981 to 09/2019. *Journal of Natural Products, 83*(3), 770-803. doi:10.1021/acs.jnatprod.9b0128

Nielsen, J. C., Prigent, S., Grijseels, S., Workman, M., Ji, B., & Nielsen, J. (2019). Comparative Transcriptome Analysis Shows Conserved Metabolic Regulation during Production of Secondary Metabolites in Filamentous Fungi. *mSystems, 4*(2). doi:10.1128/msystems.00012-19

Paterson, I., & Anderson, E. A. (2005). The Renaissance of Natural Products as Drug Candidates. *Science*, 310(5747), 451-453. doi:10.1126/science.1116364

Patridge, E. V., Gareiss, P. C., Kinch, M. S., & Hoyer, D. W. (2015). An Analysis of Original Research Contributions toward FDA-approved drugs. *Drug Discovery Today, 20*(10), 1182-1187. doi:10.1016/j.drudis.2015.06.006

Pauli, G. F., Chen, S.-N., Friesen, J. B., McAlpine, J. B., & Jaki, B. U. (2012). Analysis and Purification of Bioactive Natural Products: The AnaPurNa Study. *Journal of Natural Products, 75*(6), 1243-1255. doi:10.1021/np300066q

Pauli, G. F., Jaki, B. U., & Lankin, D. C. (2005). Quantitative 1H NMR: Development and Potential of a Method for Natural Products Analysis. *Journal of Natural Products, 68*(1), 133-149. doi:10.1021/np0497301

Pedersen-Bjergaard, S., Rasmussen, K.E. (2004). *Legemiddelanalyse*. Fagbokforlaget.

Pejin, B., Mojovic, M., & Savic, A.G. (2014) Novel Antitumor Natural Products from the Phylum Bryozoa. *Biologia Serbica (35)*(1-2), 3-14

Petersen, L.-E., Kellermann, M. Y., & Schupp, P. J. (2020). Secondary Metabolites of Marine Microbes: From Natural Products Chemistry to Chemical Ecology. In YOUMARES 9 - The Oceans: Our Research, Our Future, 159-180. Springer International Publishing.

Pettit, G. R., Herald, C. L., Doubek, D. L., Herald, D. L., Arnold, E., & Clardy, J. (1982). Isolation and Structure of Bryostatin 1. *Journal of the American Chemical Society, 104*(24), 6846-6848. doi:10.1021/ja00388a092

Rahbæk, L., Anthoni, U., Christophersen, C., Nielsen, P. H., & Petersen, B. O. (1996). Securamines and Securines, Halogenated Indole-ImidazoleAlkaloids from the Marine Bryozoan *Securiflustra securifrons*. *The Journal of Organic Chemistry, 61*(3), 887-889. doi:10.1021/jo951527a

Rahbæk, L., & Christophersen, C. (1997). Three New Alkaloids, Securamines E−G, from the Marine Bryozoan *Securiflustra securifrons*. *Journal of Natural Products, 60*(2), 175-177. doi:10.1021/np960602p

Rochfort, S. J., Moore, S., Craft, C., Martin, N. H., Van Wagoner, R. M., & Wright, J. L. C. (2009). Further Studies on the Chemistry of the Flustra Alkaloids from the Bryozoan *Flustra foliacea*. *Journal of Natural Products, 72*(10), 1773-1781. doi:10.1021/np900282j

Rose, J., Quave, C., & Islam, G. (2012). The Four-Sided Triangle of Ethics in Bioprospecting: Pharmaceutical Business, International Politics, Socio-Environmental Responsibility

and the Importance of Local Stakeholders. *Ethnobiology and Conservation, 1*. doi:10.15451/ec2012-8-1.3-1-25

Schofield, M. M., Jain, S., Porat, D., Dick, G. J., & Sherman, D. H. (2015). Identification and Analysis of the Bacterial Endosymbiont Specialized for Production of the Chemotherapeutic Natural Product ET-743. *Environmental microbiology*. doi:10.1111/1462-2920.12908

Schwaha, T. F., Handschuh, S., Ostrovsky, A. N., & Wanninger, A. (2018). Morphology of the Bryozoan *Cinctipora elegans* (Cyclostomata, Cinctiporidae) with First Data on its Sexual Reproduction and the Cyclostome Neuro-muscular System. *BMC evolutionary biology, 18*(1), 92-92. doi:10.1186/s12862-018-1206-1

Snyder, L. R., Kirkland, J. J., & Glajch, J. L. (1997). *Practical HPLC method development*. New York: Wiley.

Svenson, J. (2013). MabCent: Arctic Marine Bioprospecting in Norway. *Phytochemistry reviews: Proceedings of the Phytochemical Society of Europe, 12*(3), 567-578. doi:10.1007/s11101-012-9239-3

Tadesse, M., Strøm, M. B., Svenson, J., Jaspars, M., Milne, B. F., Tørfoss, V., . . . Haug, T. (2010). Synoxazolidinones A and B: Novel Bioactive Alkaloids from the Ascidian Synoicum pulmonaria. *Organic Letters, 12*(21), 4752-4755. doi:10.1021/ol101707u

Tadesse, M., Svenson, J., Sepčić, K., Trembleau, L., Engqvist, M., Andersen, J. H., . . . Haug, T. (2014). Isolation and Synthesis of Pulmonarins A and B, Acetylcholinesterase Inhibitors from the Colonial Ascidian Synoicum pulmonaria. *Journal of Natural Products, 77*(2), 364-369. doi:10.1021/np401002s

Taylor, P. D., Tan Shau-Hwai, A., Kudryavstev, A. B., & Schopf, J. W. (2016). Carbonate Mineralogy of a Tropical Bryozoan Biota and its Vulnerability to Ocean Acidification. *Marine Biology Research, 12*(7), 776-780. doi:10.1080/17451000.2016.1203951

Tamayo, G., Guevara, L., & Gámez, R. (2004). Biodiversity Prospecting: The INBio Experience. In *Microbial Diversity and Bioprospecting*: American Society of Microbiology. doi:10.1128/9781555817770.ch41

Thoma, F., Somborn-Schulz, A., Schlehuber, D., Keuter, V., & Deerberg, G. (2020). Effects of Light on Secondary Metabolites in Selected Leafy Greens: A Review. *Frontiers in Plant Science, 11*. doi:10.3389/fpls.2020.00497

Thomford, N. E., Dzobo, K., Chopera, D., Wonkam, A., Skelton, M., Blackhurst, D., . . . Dandara, C. (2015). Pharmacogenomics Implications of Using Herbal Medicinal Plants on African Populations in Health Transition. *Pharmaceuticals (Basel, Switzerland), 8*(3), 637-663. doi:10.3390/ph8030637

Tian, X. R., Tang, H. F., Tian, X. L., Hu, J. J., Huang, L. L., & Gustafson, K. R. (2018). Review of Bioactive Secondary Metabolites from Marine Bryozoans in the Progress of New Drugs Discovery. *Future Medicinal Chemistry, 10*(12), 1497-1514. doi:10.4155/fmc-2018-0012

Vacher, M., Fdez. Galván, I., Ding, B.-W., Schramm, S., Berraud-Pache, R., Naumov, P., . . . Lindh, R. (2018). Chemi- and Bioluminescence of Cyclic Peroxides. *Chemical Reviews, 118*(15), 6927-6974. doi:10.1021/acs.chemrev.7b00649

Varbanov, P.H., Kuttler, F., Banfi, D., Turcatti, G., & Dyson, P.J. (2017). Repositioning Approved Drugs for the Treatment of Problematic Cancers Using a Screening Approach. *PLOS ONE, 12*(2), https://doi.org/10.1371/journal.pone.0171052

Ventola, C. L. (2015). The antibiotic resistance crisis: part 1: causes and threats. *Pharmacy and Therapeutics*, 40(4), 277-283. PMID: 25859123

Weyrich, L. S., Duchene, S., Soubrier, J., Arriola, L., Llamas, B., Breen, J., . . . Cooper, A. (2017). Neanderthal Behaviour, Diet, and Disease Inferred from Ancient DNA in Dental Calculus. *Nature, 544*(7650), 357-361. doi:10.1038/nature21674

Wilm, M. (2011). Principles of Electrospray Ionization. *Molecular & Cellular Proteomics, 10*(7), M111.009407. doi:10.1074/mcp.m111.00940

Wood, T. S. (2015). Chapter 16 - Phyla Ectoprocta and Entoprocta (Bryozoans). In J. H. Thorp & D. C. Rogers (Eds.), *Thorp and Covich's Freshwater Invertebrates (Fourth Edition)* (pp. 327-345). Boston: Academic Press

7 Appendix

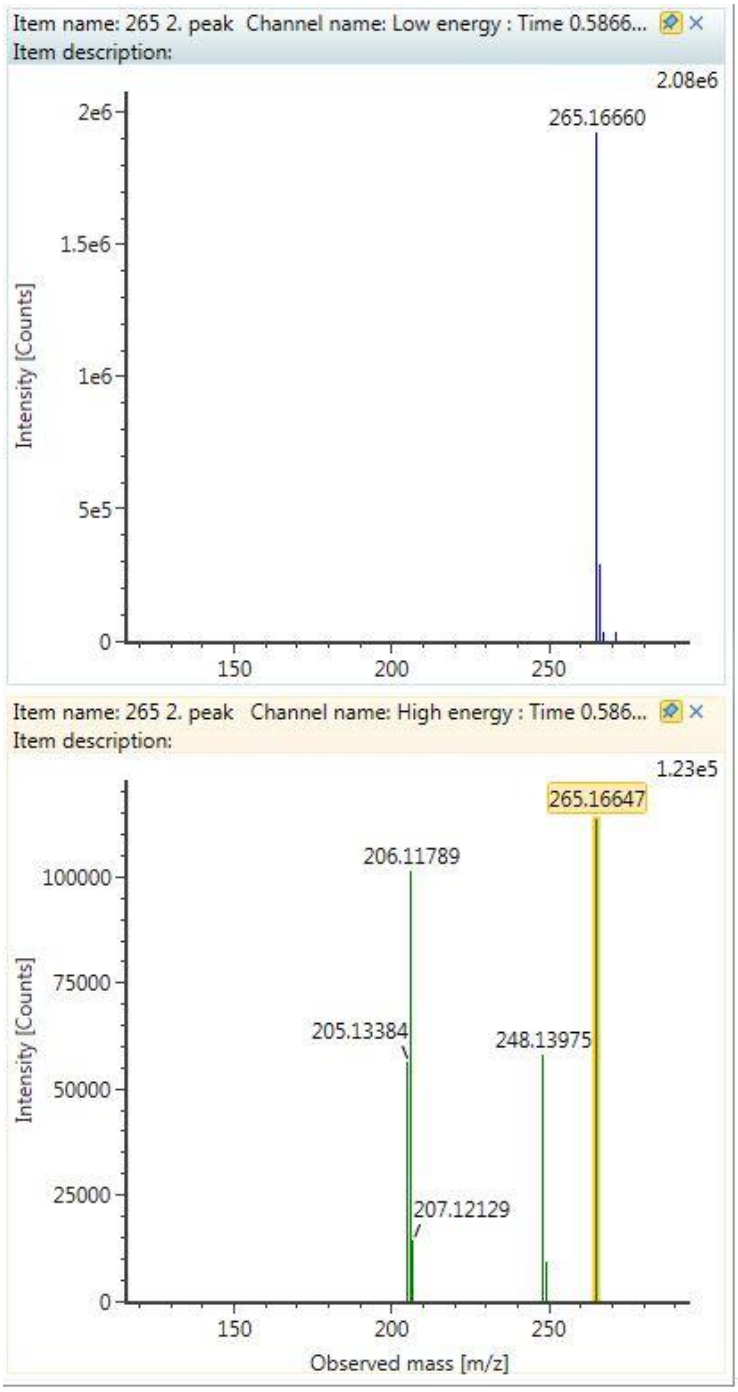

Figure A1 - Low and high energy spectra at 60 eV for MBC-342. *Two fragments (m/z 248.13975 and 206.11789) was used to elucidate the structure of MBC-342.*

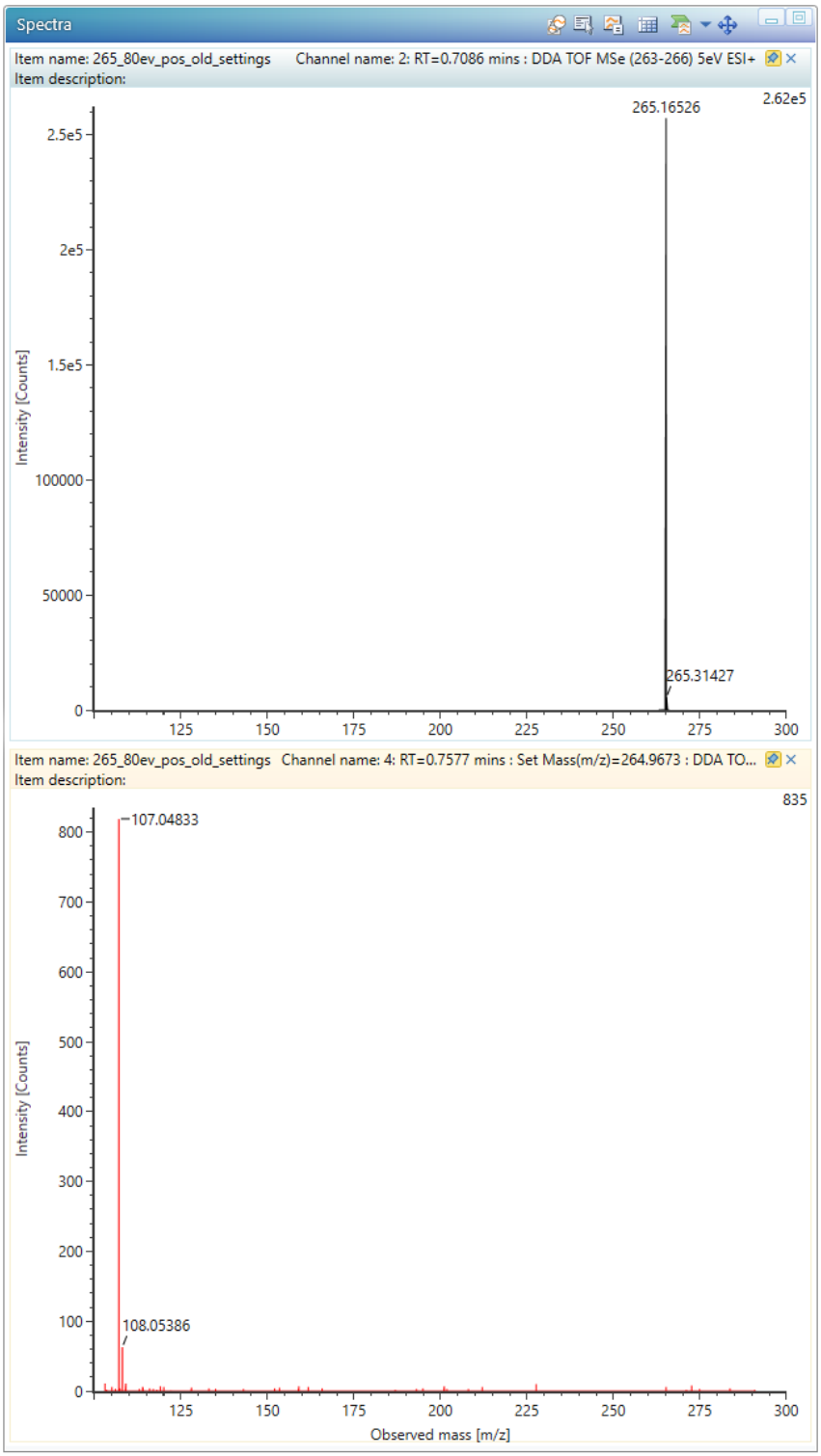

Figure A2 - Low and high energy spectra at 80 eV for MBC-342. *Fragment m/z 107.04833 was used to elucidate the structure of MBC-342.*

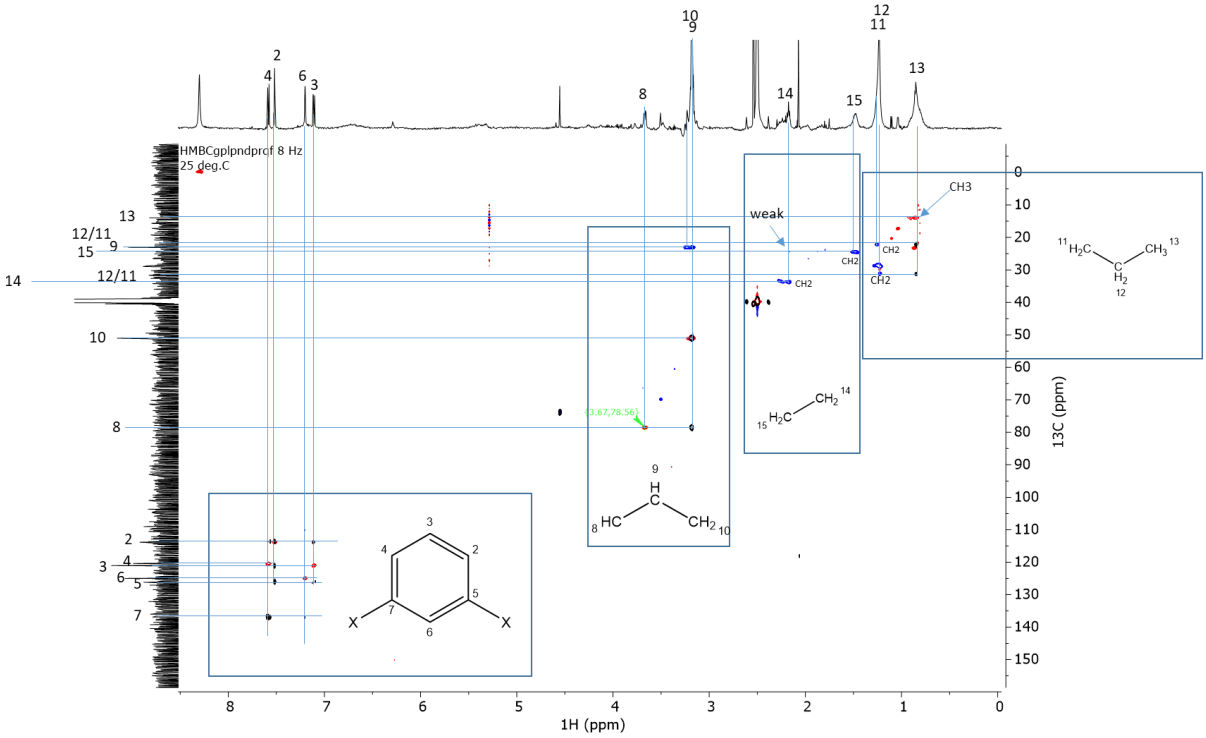

Figure A3 - HSQC and HMBC data of MBC-339 with elucidated substructures.

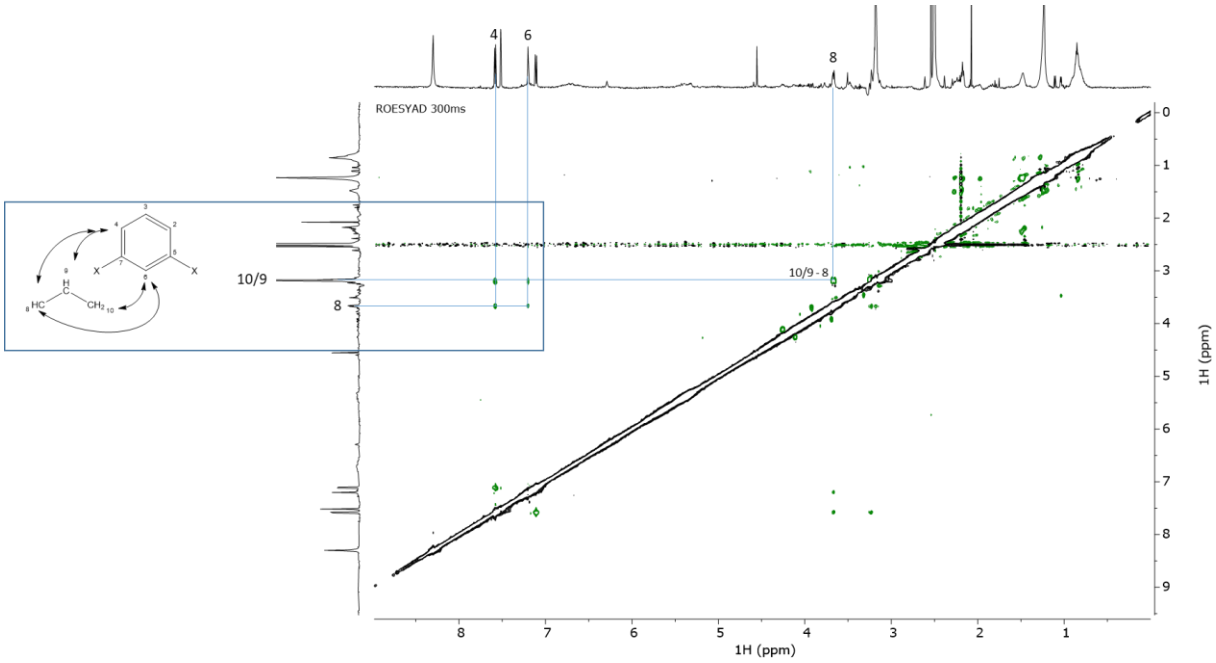

Figure A4 - ROESY data connecting two of the MBC-339 substructures.

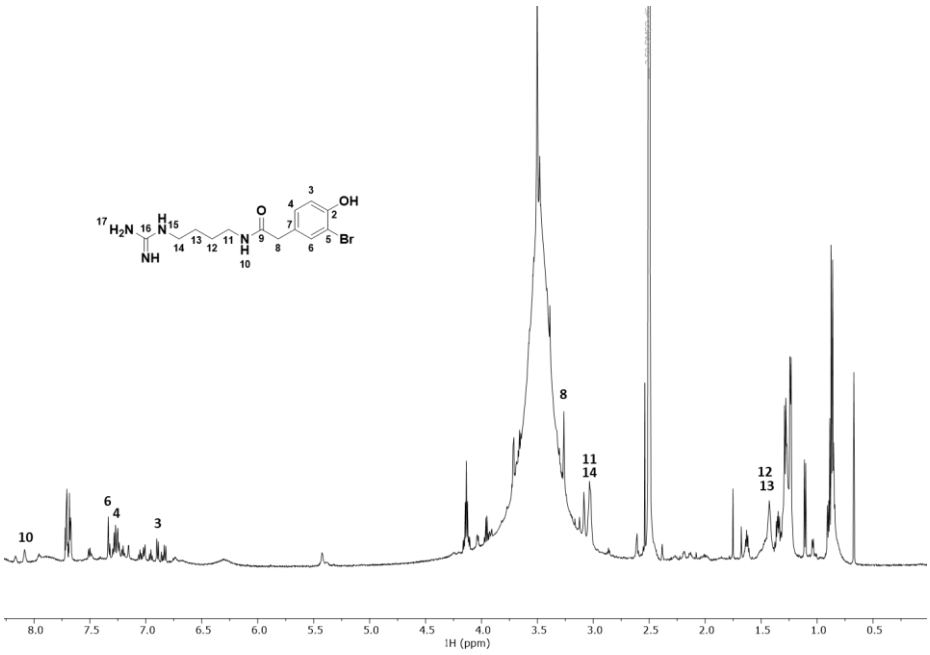

Figure A5 - ^{1}H NMR spectrum of MBC-340.

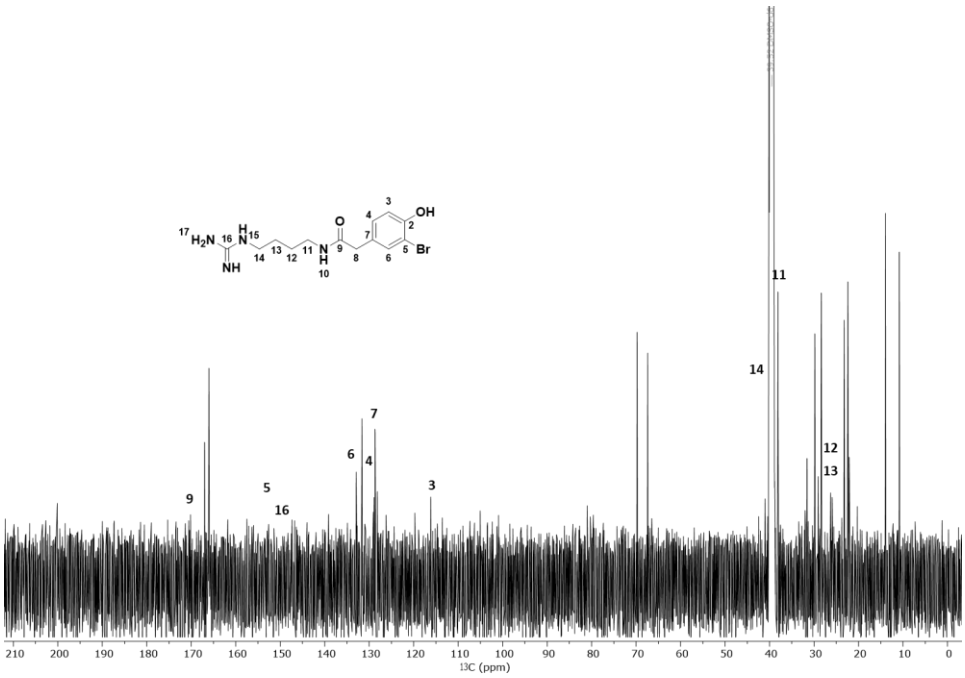

Figure A6 - ^{13}C NMR spectrum of MBC-340.

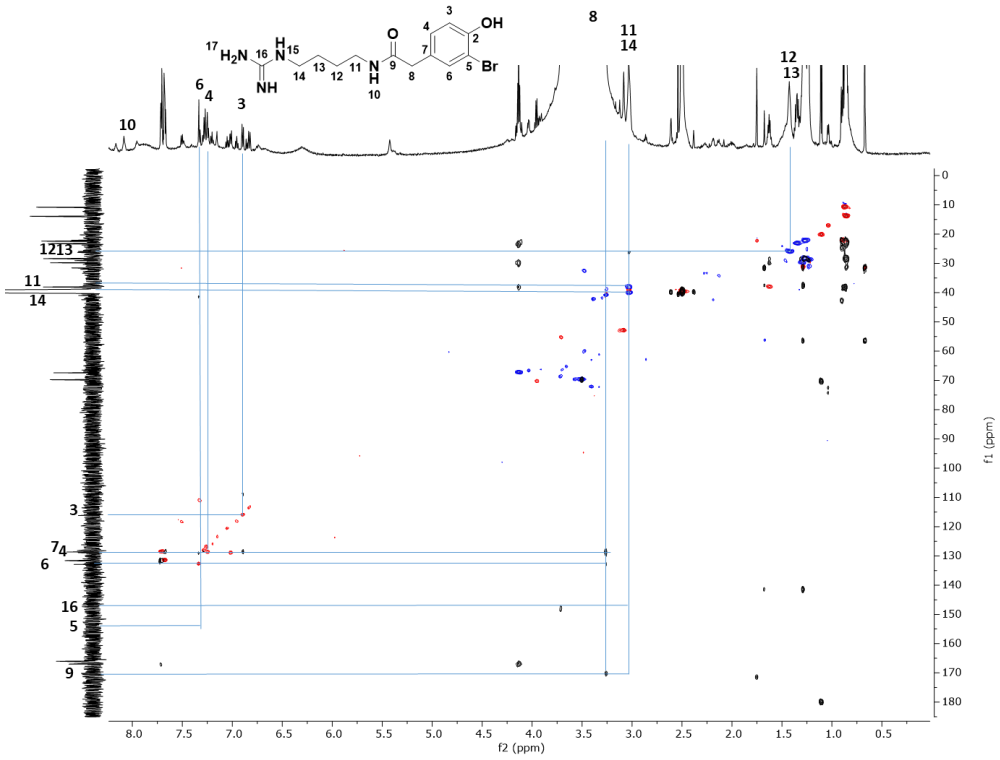

Figure A7 - HMBC + HSQC spectrum of MBC-340.

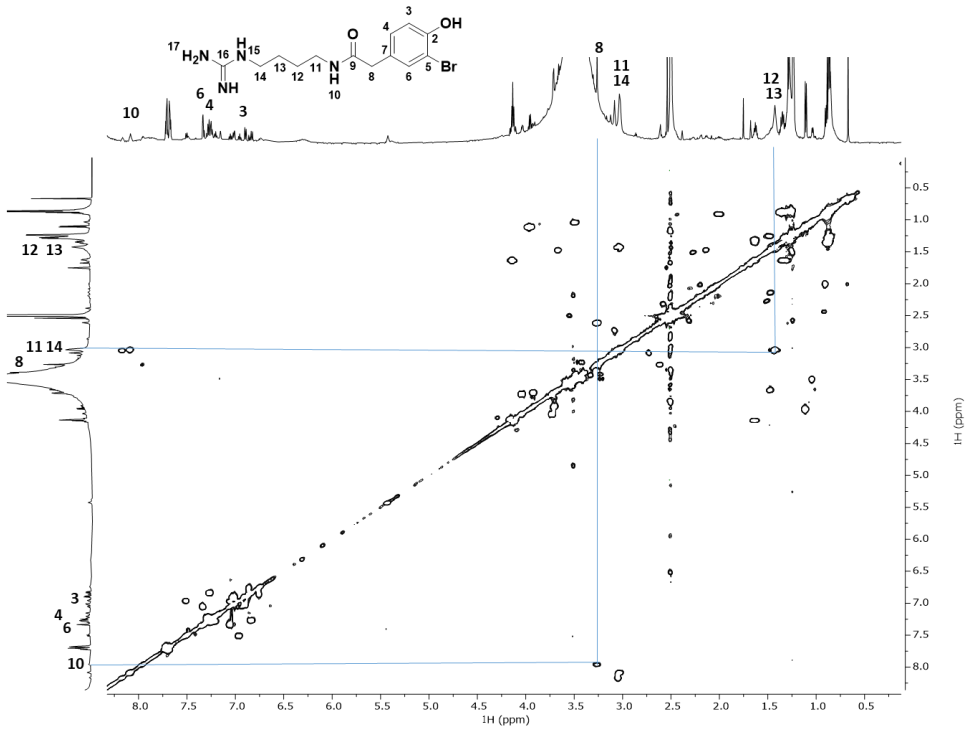

Figure A8 - COSY spectrum of MBC-340.